

AN ABSTRACT OF THE THESIS OF

R. MARTIN OLIVERA for the degree of MASTER OF SCIENCE
in OCEANOGRAPHY presented on 17 DECEMBER 1982

Title: A COMPLEX DISTRIBUTION OF WATER MASSES AND RELATED
CIRCULATION OFF NORTHERN CALIFORNIA IN JULY 1981

Abstract approved: Redacted for privacy
Adriana nuyeri

Hydrographic observations were made off Northern California from 1 July to 14 July, 1981. The CTD data and complementary satellite information showed a very complex distribution of surface temperature and salinity. These features penetrated to subsurface layers. Two surface water masses were identified off Pt. Arena (~39°N), separated by a strong density front. One was warm-fresh, influenced by the Columbia River Plume; the second was cooler and saline, of subsurface origin. A third surface water mass was detected near the coast, farther south (~38°40'N and off Half Moon Bay) with relatively high temperature and salinity, probably the result of local heating upon upwelled waters. The currents were approximately geostrophic and followed a meandering pattern. The main flow was along the boundary between the water masses. The highest velocities were computed at the surface in the frontal area. Northwestward flow was observed offshore, from the surface to at least 300 db. Indications of a weak, discontinuous, poleward, subsurface flow were found near the continental slope at different locations.

A Complex Distribution of Water Masses
and Related Circulation off Northern
California in July 1981

by

Ricardo Martin Olivera

A THESIS

submitted to

Oregon State Universtiy

in partial fulfillment of
the requirements for the
degree of
Master of Science

Completed 17 December 1982

Commencement June 1983

APPROVED:

Redacted for privacy

Associate Professor of Oceanography in charge of major

Redacted for privacy

Dean of School of Oceanography

Redacted for privacy

Dean of Graduate School

Date thesis is presented 17 DECEMBER 1982

Typed by Dana Wimer for R. MARTIN OLIVERA

ACKNOWLEDGEMENTS

I thank Jane Hoyer, my major professor, for her constant help, support and encouragement. I also would like to express my thanks to the people who participated in the data collection and processing: Rich Schramm, Dennis Barstow, Henry Schaechterle and Jane Fleischbein and Bill Gilbert, who in addition, drafted the figures in this work. Michael Kosro kindly provided the chart with Doppler Acoustic Log velocities. Kathryn Kelly and Larry Breaker provided the satellite images. Dana Wimer typed early drafts and the final manuscript.

I thank Jim Richman for his valuable comments and ideas.

My special thanks to Jenny Wiser for without her understanding and unlimited patience I would not have made it.

My stay at Oregon State University was supported by the Organization of the American States. Hydrography in the Coastal Ocean Dynamics Experiment is supported by the National Science Foundation through grant OCE-8014943.

TABLE OF CONTENTS

<u>Chapter</u>	<u>Page</u>
I. Introduction.	1
II. The Observations.	6
III. Results.	10
IV. Discussion.	
A. The Water Masses.	25
B. The Distribution of Water Masses and Related Circulation.	35
C. Large Scale Circulation.	42
D. Comparison of Geostrophic and Observed Currents.	47
V. Summary and Conclusions	50
VI. Bibliography	52

LIST OF FIGURES

<u>Figure</u>	<u>Page</u>
1. Satellite infrared radiometer images for (a) <u>left</u> 0900 a.m. PDT, 26 June 1981 and (b) <u>right</u> 0800 p.m. PDT, 8 July 1981.	3
2. Sea Surface Thermal Analysis maps for (top) 1 July 1981 and (bottom) 9 July 1981, transmitted by the National Earth Satellite Service, Redwood City, California. The cruise track for the offshore survey is superimposed.	4
3. Position of CTD stations during the offshore survey near the CODE region, by the R/V Wecoma, 4-10 July 1981.	7
4. Time series of wind speed and direction as observed during CTD stations between 2 July and 11 July 1981. The mean wind speed was 19 knots and the mean wind direction was 328°T ($N = 103$).	8
5. Maps of sea surface temperature (bottom) and salinity (top) superimposed on the satellite image of 0320 Z, 8 July 1981.	11
6. Temperature-Salinity plots: (a) at the sea surface, (b) at 50 db, (c) at 100 db and (d) at 200 db. Dots and triangles represent stations with bottom depth greater and less than 1000 db respectively. r = correlation coefficient, N = number of observations.	13
7. The horizontal distribution of temperature and salinity at selected levels: the sea surface, 50 db, 100 db and 200 db. Contour intervals are 1°C and $0.25^{\circ}/\text{‰}$ except for 200 db (0.5°C and $0.10^{\circ}/\text{‰}$).	17
8. The horizontal distribution of potential density anomaly (σ_{θ}) and the dynamic height relative to 500 db at selected levels: the sea surface, 50 db, 100 db and 200 db. Contour intervals are 0.25 g/l and 2 dyn cm, except for 200 db (0.10 g/l).	20
9. T-S diagrams of Stations KP58, KP59 and KP60 made in July 1967 (bigger dots in the inset); and those of Stations 34 and 49 made in July 1981. The inset shows the sea surface salinity off Oregon in July 1967 (after Cissell, 1969).	28

<u>Figure</u>	<u>Page</u>
10. Vertical sections of temperature and salinity along the CODE Central Line for 4-5 July and for 8 July 1981.	32
11. T-S diagram of Station 22 up to 200 m and that constructed with surface values of Stations 71 through 80.	33
12. T-S diagrams of stations occupied within the warm and fresh water (Station 36), within the cool saline water (Station 75), and within the warm and saline water (Stations 9 and 106). Additional diagrams for Stations 62 and 84 lie within a transition area.	34
13. Temperature-Salinity (T-S) and Temperature-Geostrophic Velocity (T-Vg) sections for: (a) Stations 34-24; (b) Stations 34-43; (c) Stations 43-52; (d) Stations 52-64; and (e) Stations 9-24. The geostrophic velocity is with respect to 500 db (in cm/sec). Dashed lines represent temperature at the sea surface and at 500 db.	39
14. Mean dynamic topography of the sea surface off California relative to 500 db during July. Contour intervals are 0.02 dyn meters (after Hickey, 1979). The square region represents the CODE 1, Leg 7 survey area.	44
15. Geostrophic velocity profiles relative to 500 db for pairs of stations near the continental slope. Shaded areas and negative values represent poleward and equatorward flow respectively.	45
16. Geostrophic velocity (cm/sec) at the sea surface relative to 500 db between distant stations.	46
17. Maps of current velocity: (top) as measured by a Doppler Acoustic Log (courtesy of Michael Kosro, Scripps Institute of Oceanography); (bottom) as observed in the dynamic height of 30/500 db (contour intervals are 2 dyn cm).	49

A Complex Distribution of Water Masses
and Related Circulation off Northern
California in July 1981

I. Introduction

During 1981 and 1982, the Coastal Ocean Dynamics Experiment conducted a series of hydrographic cruises to study the near-shore waters off northern California between Pt. Arena and Pt. Reyes. The main purpose of these cruises was to study the response of shelf waters to the changing wind stress, but an important second purpose was to study the oceanic environment just seaward of the shelf. The first detailed survey of the offshore waters near Pt. Arena was conducted during Leg 7 of CODE-1, the first Coastal Ocean Dynamics Experiment, in July 1981. This thesis describes and discusses the results of this offshore survey.

The design of the survey was influenced by a number of factors: the satellite infrared images available prior to the cruise; maps of sea surface temperature available during the cruise; the need to complete the survey within several days, so that the results would be at least quasisynoptic; and the need to make sections along standard Code lines across the shelf between Pt. Arena and Pt. Reyes, and off Half Moon Bay.

Just prior to the cruise, which departed from Newport, Oregon on 1 July 1981, colleagues at Scripps Institution of Oceanography provided us with satellite infrared radiometer images for 26 and 27 June. Both of these showed a band of cold water present all along the coast, generally about 50 miles wide. In addition, the images

showed a few tongues or plumes of cold water extending much farther out to sea. One such cold tongue extended more than 100 miles offshore from Pt. Arena; it seemed to have a very sharp boundary along its southern edge, and a more gradual northern boundary (Figure 1a). There was no discernible change in its position between the times the images were taken at 0900 PDT on 26 June and 0900 PDT on 27 June. Unfortunately, the region was covered by cloud from 30 June through 5 July, so no further satellite images were available until 6 July (Kelly, 1981).

During the cruise, we received facsimile maps of the Sea Surface Thermal Analysis transmitted by the National Earth Satellite Service once per week. These maps are based partly on the satellite infrared images and partly on ship reports (Larry Breaker, personal communication). The portion of the 1 July map near Pt. Arena (Figure 2a) is in close agreement with the 26 June satellite image (Figure 1a).

Our intent in designing the offshore survey was to cross at least the sharp southern boundary of the cold plume. If, as we expected, the cold plume were advected southward, we would also cross the more diffuse northern boundary. We chose to begin with an offshore-directed section along the Code Central Line (Stations 9-24 in Figure 3), and then to zig-zag our way back toward the coast, hoping to cross the cold plume as we did so (Figure 1 and 2). In this way, we hoped to determine whether there were subsurface features in the temperature, salinity, density and current fields that were associated with the cold surface water. In actuality, of course, the sea surface temperature distribution did not remain

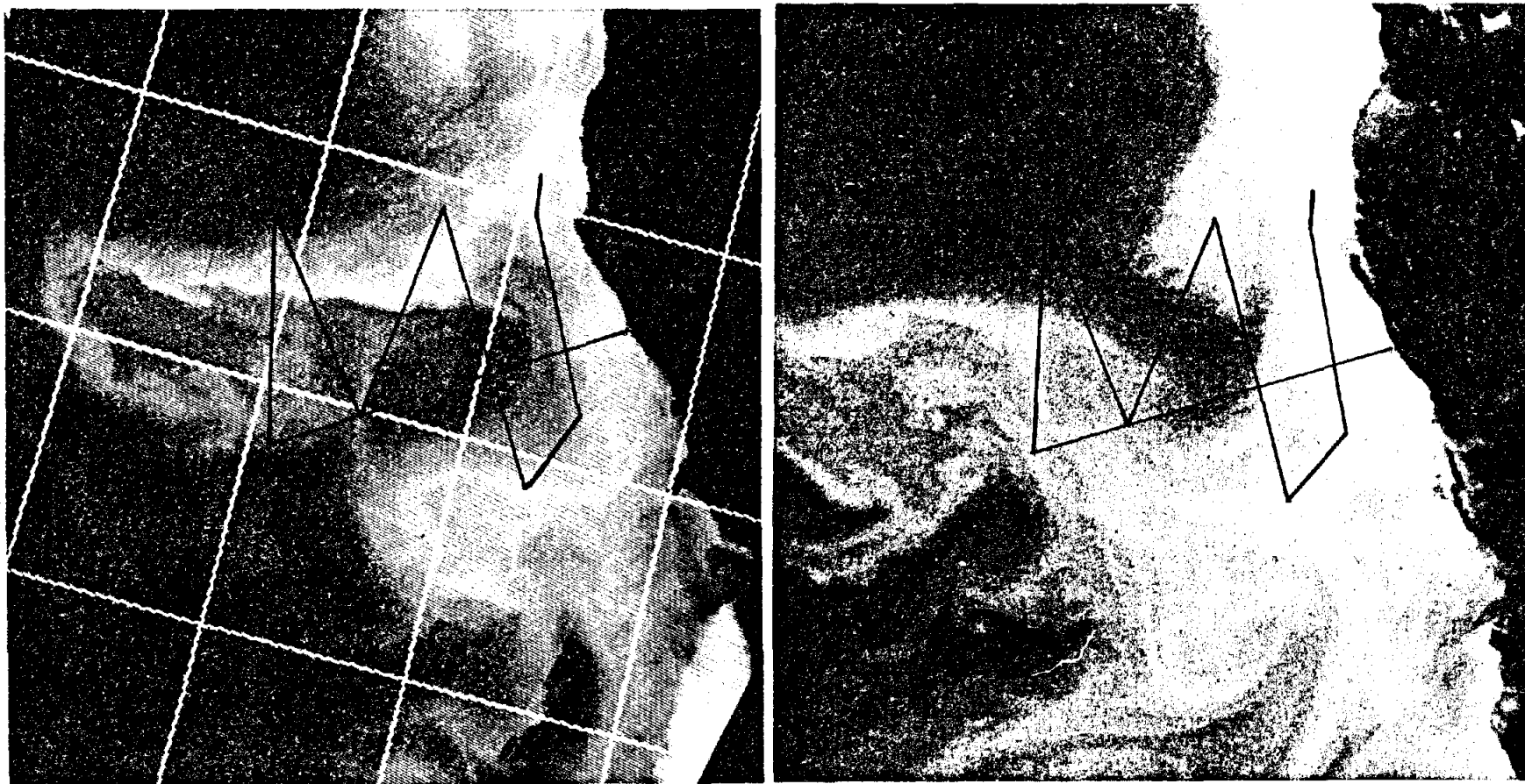


Figure 1. Satellite infrared radiometer images for (a) left, 0900 a.m. PDT, 26 June 1981 and (b) right, 0800 p.m. PDT, 8 July 1981.

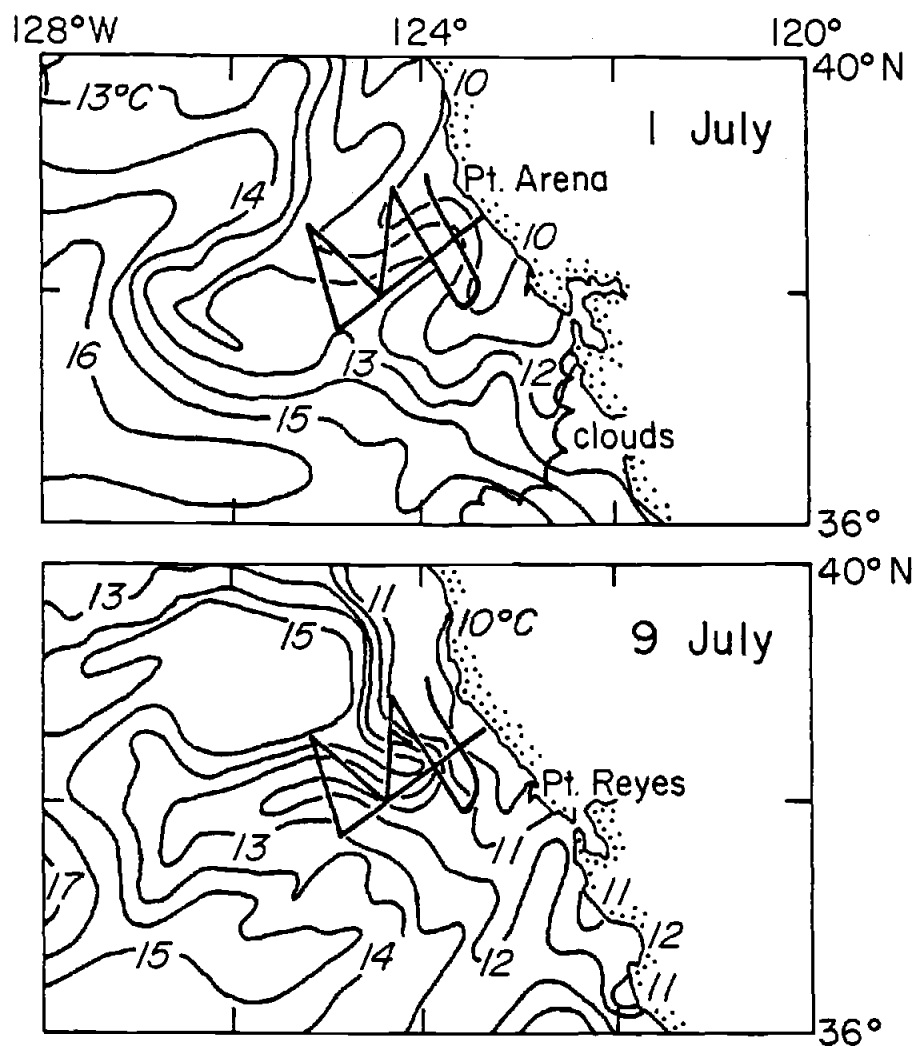


Figure 2. Sea Surface Thermal Analysis maps for (top) 1 July 1981 and (bottom) 9 July 1981, transmitted by the National Earth Satellite Service, Redwood City, California. The cruise track for the offshore survey is superimposed.

constant after 26 June - in fact, the satellite infrared images indicate it changed quite drastically between 26 June and 8 July (Figure 1). The Sea Surface Thermal Analysis map for 9 July (Figure 2), in good agreement with the 8 July satellite image (Figure 1), shows a tongue of relatively warm water extending southeastward across the central portion of the survey track. Our survey pattern was not optimized for this distribution; nevertheless, it would result in sampling of both warm and cold water masses, both near-shore and offshore cold water, and several transects across a strong surface temperature front (Figure 1b). In the remainder of this thesis, we will describe the results of the offshore survey, and discuss the observed distributions of temperature, salinity, and density, the water masses present, and the associated circulation patterns.

II. The Observations

The offshore survey began on 4 July with an extended section (Stations 9 to 24) along the Code Central Line. We then made a section heading approximately north-northeastward and continuing until surface waters were fairly uniformly warm several stations in a row. We continued to zig-zag toward the coast, making turns at Stations 34, 43, 52 and crossing the Central Line with Station 59. We continued southeastward roughly along the 1000 fm isobath. We began a section along the 100 fm isobath but interrupted it to repeat the inshore part of the Central Line because the winds had changed since the first occupation. We then continued along the 100 fm line, before occupying a standard section off Pt. Arena (Stations 92-98) on 9 July. These stations essentially completed the offshore survey. Additional stations (100-103) were made near the 1000 fm isobath on our way to occupy a standard section (Stations 103-111) off Half Moon Bay on 10 July. These stations (i.e. 100-111) were not originally intended to be included in the offshore survey, but they are included in this analysis. The station distribution is shown in Figure 3.

The entire survey (Stations 9-111) was completed between 1950 Z, 4 July and 1700 Z, 10 July, i.e. in just under six days. The wind direction was nearly steady throughout the survey: it varied only between 280° and 350° T, and was usually between 320° and 340° T (Figure 4). Winds were quite weak (< 10 kts) during the first day, but increased during the second day and remained high (~ 25 kts) for the remainder of the survey (Figure 4). The inshore end of the

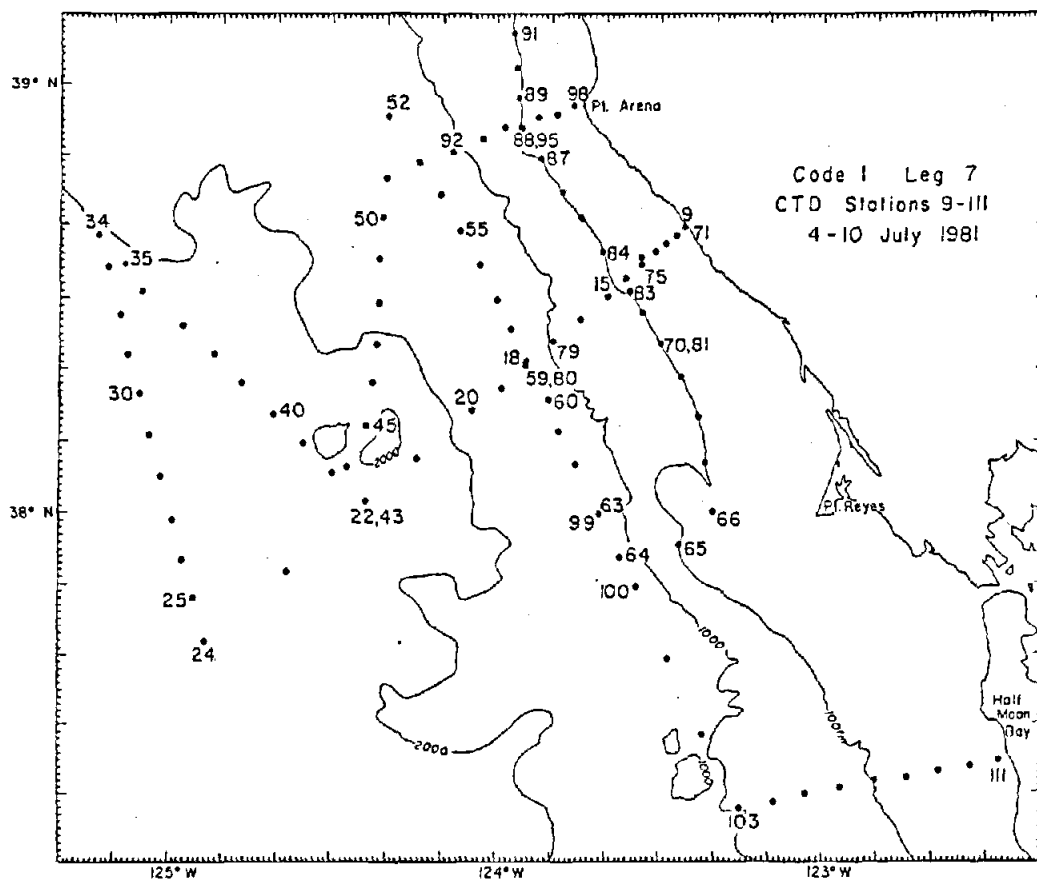


Figure 3. Position of CTD stations during the offshore survey near the CODE region by the R/V Wecoma, 4-10 July 1981.

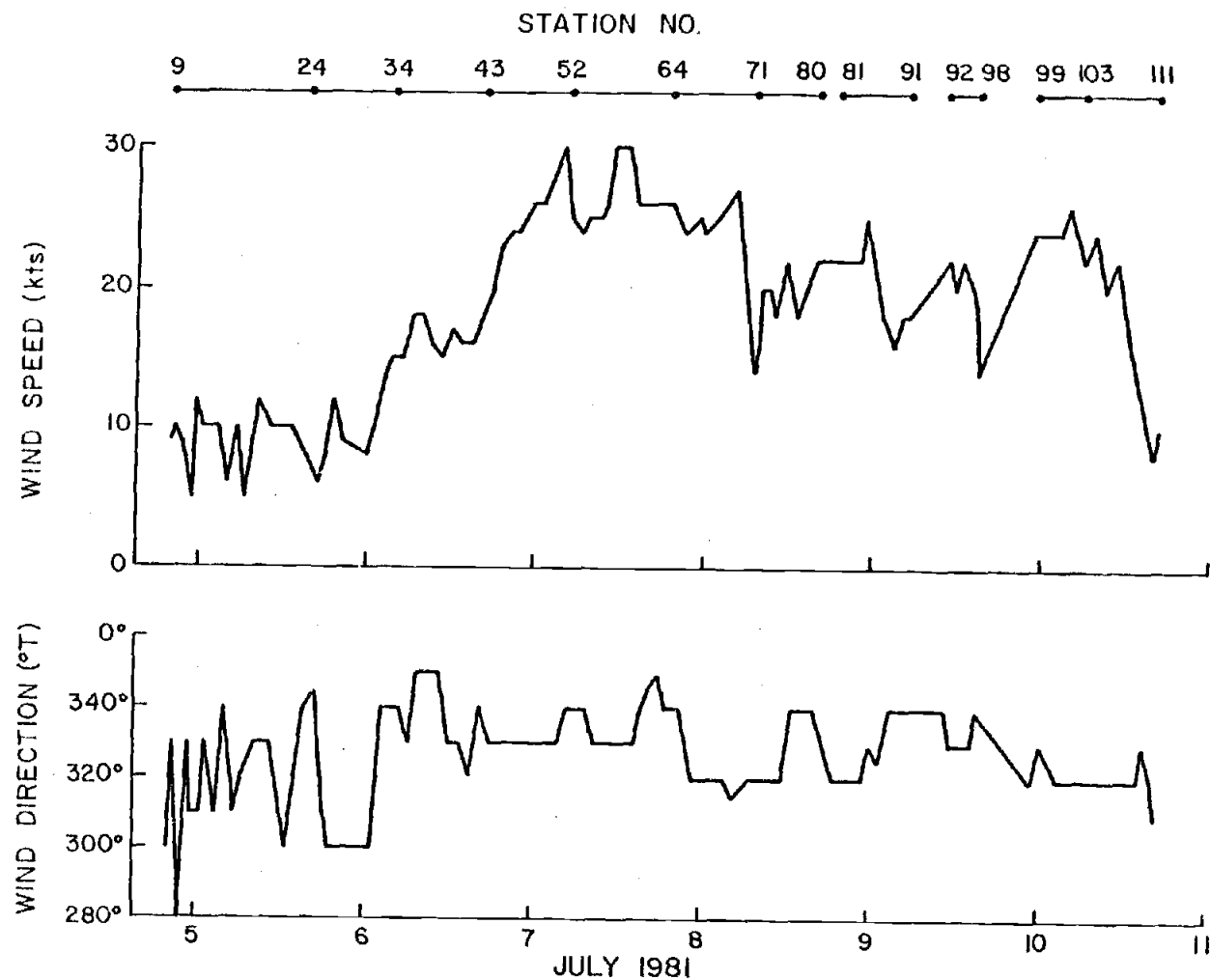


Figure 4. Time series of wind speed and direction as observed during CTD stations between 2 July and 11 July, 1981. The mean wind speed was 19 knots and the mean wind direction was 328°T (N= 103).

Code Central Line was sampled twice - once at the beginning when winds were weak, and once near the end of the survey when winds were strong. Since strong winds dominated the survey, the later data (i.e. Stations 71-80) are used in the analysis of horizontal distributions of properties.

At each station, we made a CTD cast to 500 db (or to within 10-20 m of the bottom over the upper continental slope and shelf) using a Neil Brown Mark III-B CTD system. The system measures conductivity, temperature and pressure, with a complete scan every 32 milliseconds. In situ calibration data was obtained from a Niskin bottle hung about 2 m above the CTD sensors. The CTD conductivity data were adjusted to agree with the sample data before the data were processed to yield 1 db averages of the temperature and salinity. Details of the sampling and data processing procedures are described in the data report for this cruise (Olivera et al., 1982).

III. Results

The distribution of sea surface temperature measured during the survey shows low temperature values ($< 10^{\circ}\text{C}$) near the coast between Pt. Arena and Pt. Reyes (Figure 5); surface temperature generally increases seaward, from $< 10^{\circ}\text{C}$ at the coast to $> 12^{\circ}\text{C}$ offshore. The surface temperature distribution is in good agreement with the 8 July infrared satellite image (Figure 5a): the 13°C isotherm lies nearly along the boundary between the dark (warm) and light (cold) areas in the satellite image; isotherms are packed close together where the boundary appears to be sharp, and are farther apart where the boundary appears to be more diffuse. The agreement is not perfect - e.g. off Pt. Arena, the temperature front is about ten miles farther offshore in the satellite image than in the CTD survey data; this difference is not surprising since the stations in this region (i.e. 49-52) were made a full day before the satellite image. Similarly, the coldest water in the farthest offshore portion of the survey seems to lie farther north in the CTD data (obtained 5-6 July) than in the 8 July satellite image. The stations occupied on 8 July (67-85) all agree well with the satellite image: Station 80, with a surface temperature of 13°C lies right on the boundary between dark and light areas; the remainder (i.e. Stations 67-79 and 81-84) all have surface temperatures of 11°C or less and all lie within the light area along the coast.

The surface salinity distribution is similar to the surface temperature distribution (Figure 5), with highest salinity adjacent

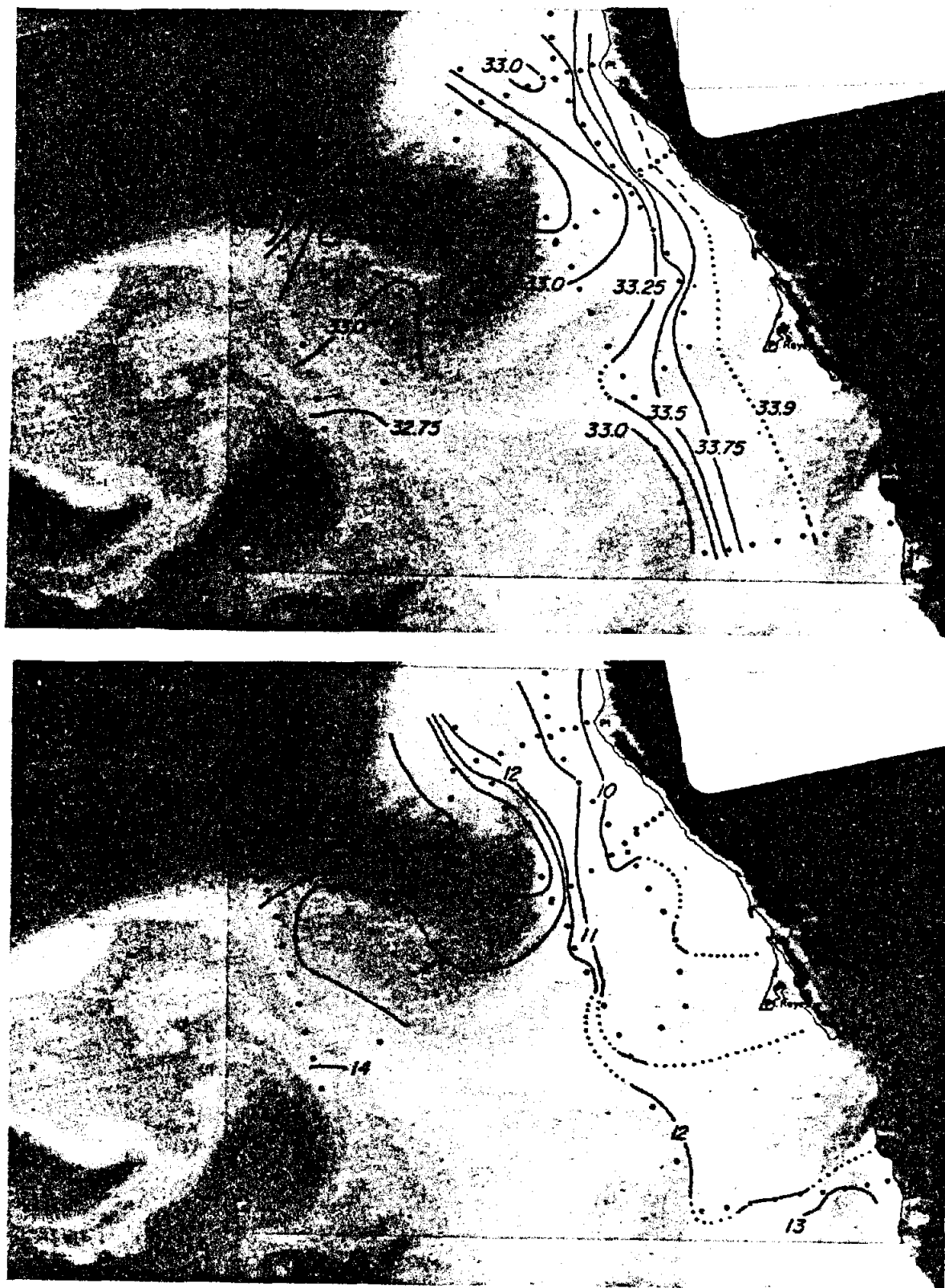


Figure 5. Maps of sea surface salinity (top) and temperature (bottom) superimposed on the satellite image of 0320 Z, 8 July 1981.

to the coast and generally decreasing offshore. The fronts between light and dark areas in the satellite image seem to correspond with salinity gradients as well as temperature gradients. Low surface salinities are associated with high surface temperatures and vice versa, except that some stations off Half Moon Bay have high salinity surface water that is relatively warm (Figure 5, 6a). The strongest salinity gradients, between 33.25‰ and 33.75‰ , seem to be associated with only weak temperature gradients (Figure 5).

The temperature and salinity fronts which separate the dark area in the northwest corner from the remainder (Figure 5) reinforce each other to produce an even stronger density front (Figure 8). The lighter surface water ($\sigma_\theta < 24.25$) is characterized by temperatures greater than 14°C and salinities below 32.75‰ , whereas the denser ($\sigma_\theta > 24.75$) water has temperatures below 13°C and salinities above 32.8‰ (compare Figure 7 and 8). At 50 db, the horizontal gradients in temperature, salinity and density are all weaker (Figure 7 and 8); the density front lies about 10 km farther north, at $38^\circ 20'\text{N}$, $125^\circ 10'\text{W}$. There is very little water with temperature greater than 13°C or salinity less than 32.75‰ at this depth (Figure 6b); the coastal band has temperatures below 9°C and salinities above 33.9‰ . The lowest salinities on the 50 db surface seem to lie directly under the low salinity water at the surface, but the warm ($> 11^\circ\text{C}$) water at 50 db extends farther south than the warmest surface water ($T > 14^\circ\text{C}$). No trace of the warm-fresh ($T > 12^\circ\text{C}$, $S < 32.8\text{‰}$) water is found at 100 db (Figure 7). Although gradients at this depth are considerably weaker, the

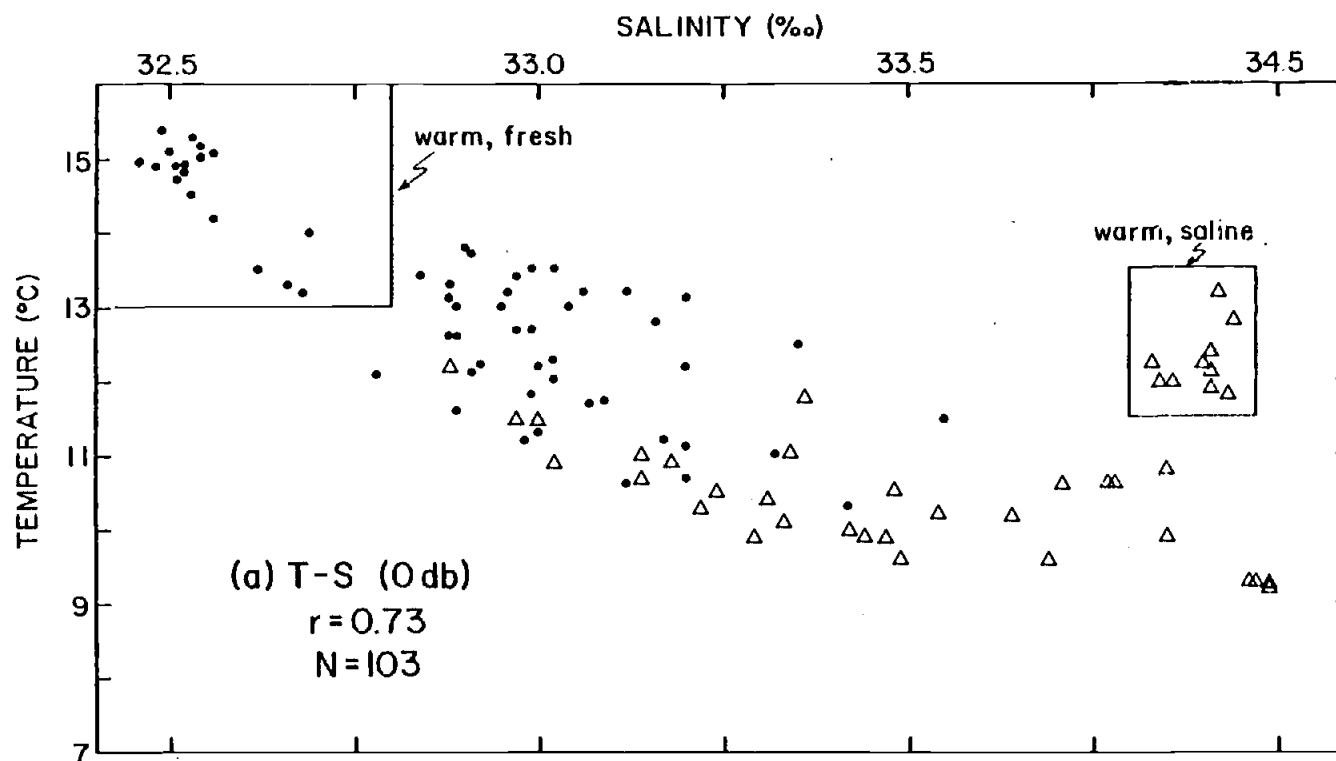


Figure 6

Temperature-Salinity plots at the sea surface. Dots represent stations with bottom depth greater than 1000 db,; triangles represent stations with bottom depth less than 1000 db. r = correlation coefficient, N = number of observations.

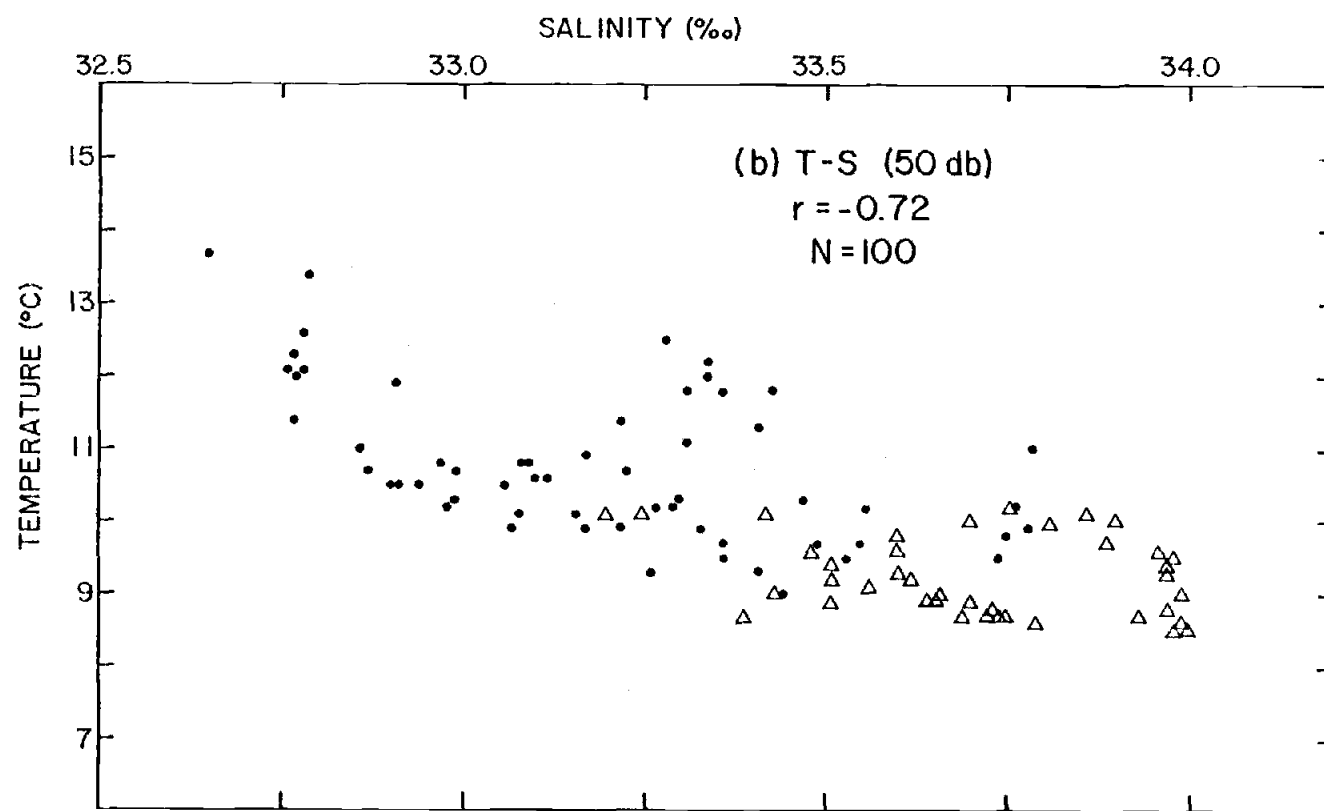


Figure 6. (cont.)

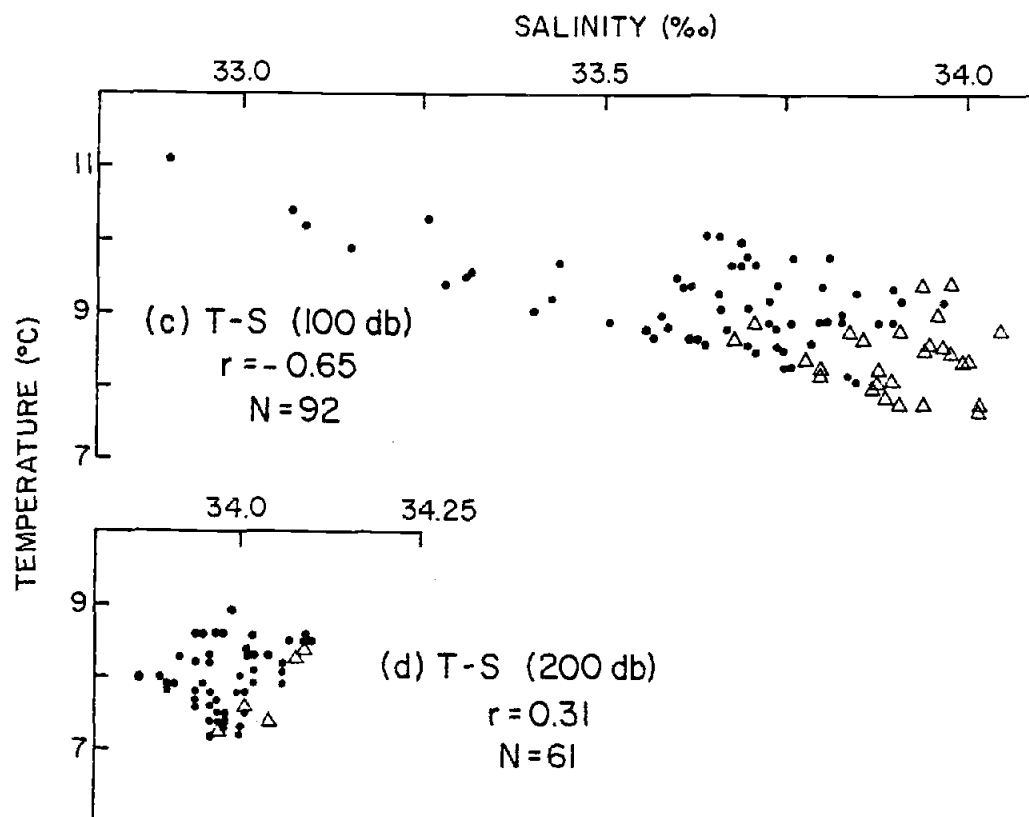


Figure 6. (cont.)

Figure 7

The horizontal distribution of temperature and salinity at selected levels: the surface, 50 db, 100 db and 200 db. Contour intervals are 1°C and 0.25 ‰ except for 200 db (0.5°C and 0.10 ‰).

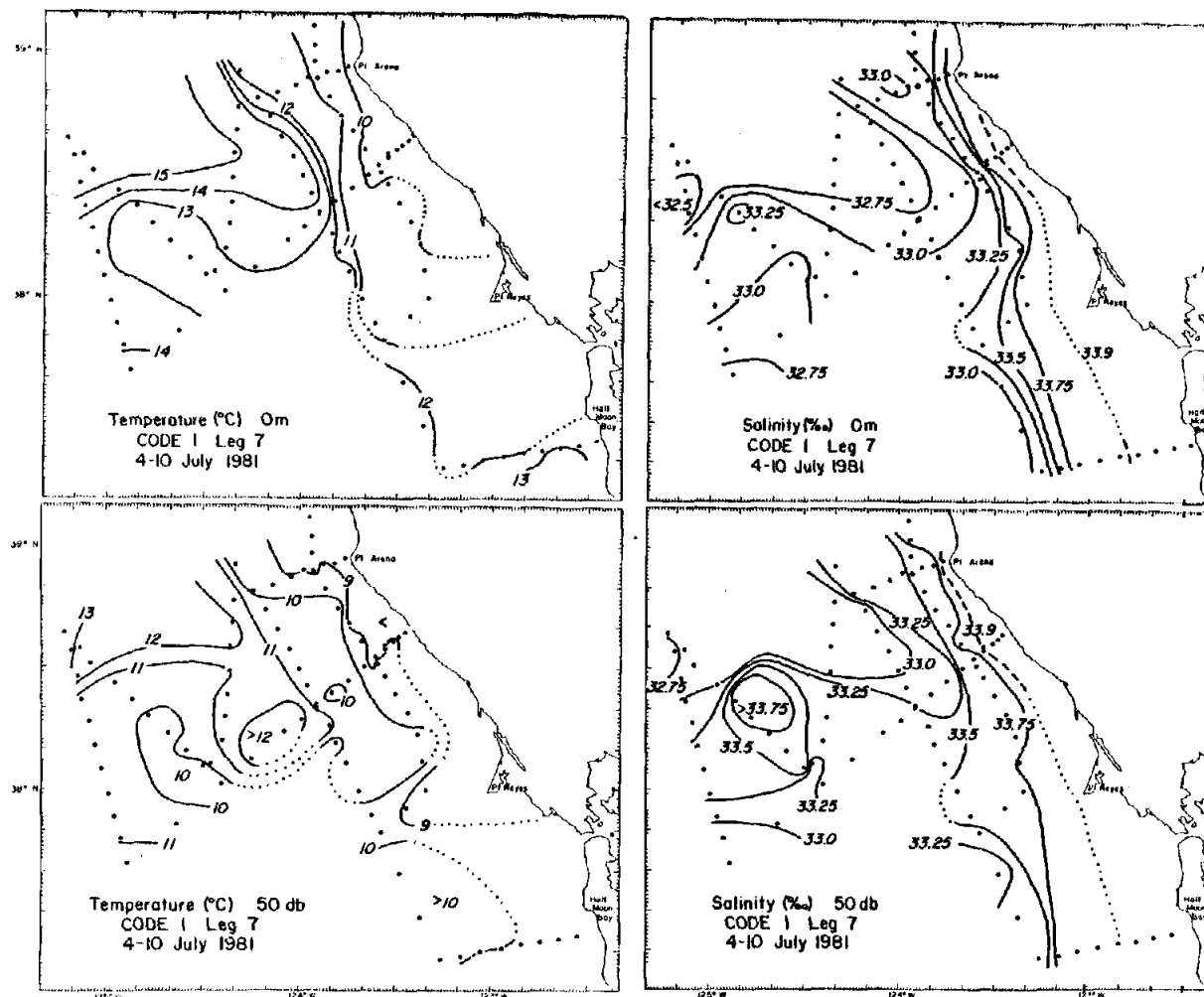


Figure 7

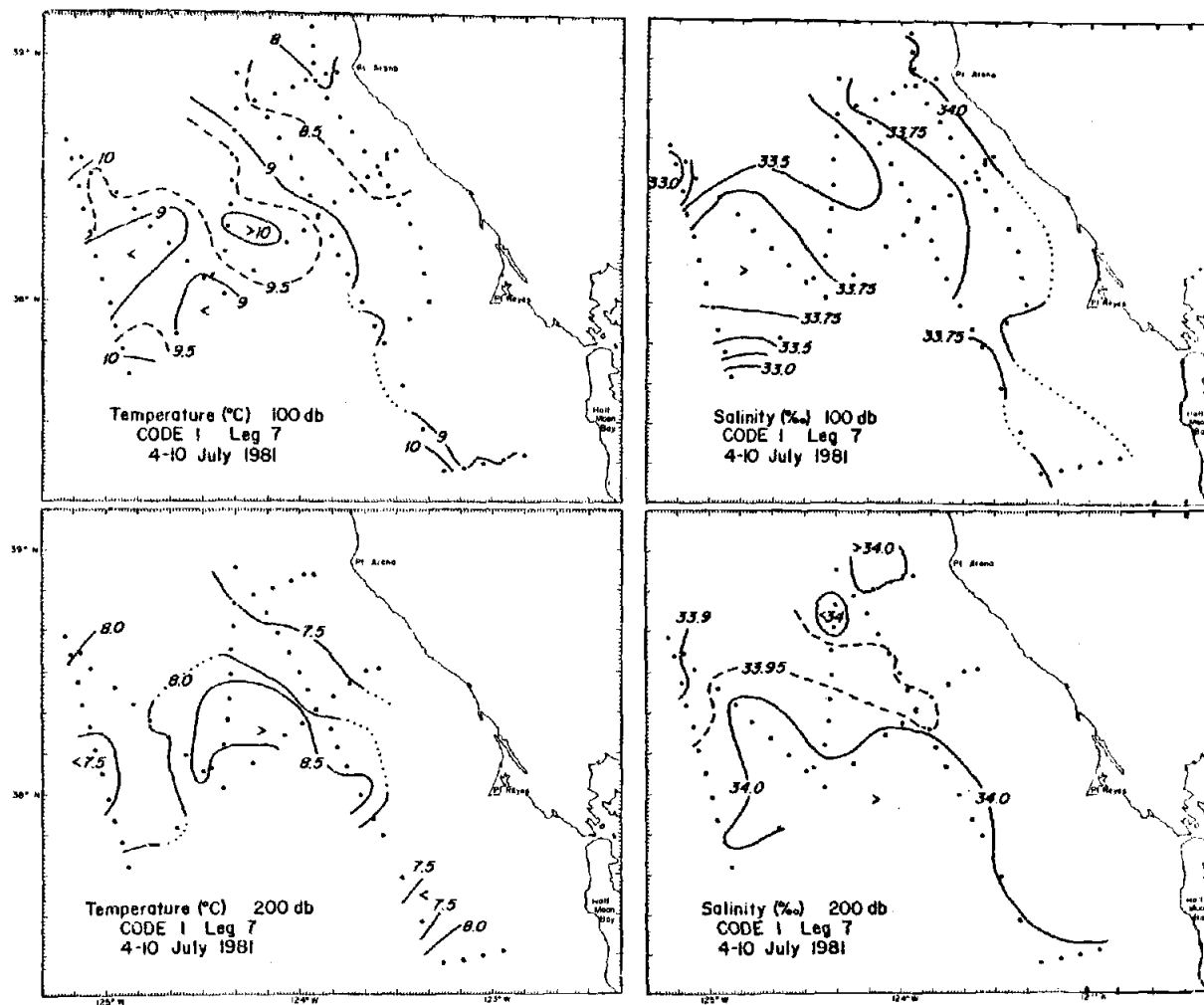


Figure 7 (cont.)

Figure 8

The horizontal distribution of potential density (σ_θ) and the dynamic height relative to 500 db at selected levels: the surface, 50 db, 100 db and 200 db. Contour intervals are 0.25 g/l and 2 dyn cm, except for 200 db (0.10 g/l).

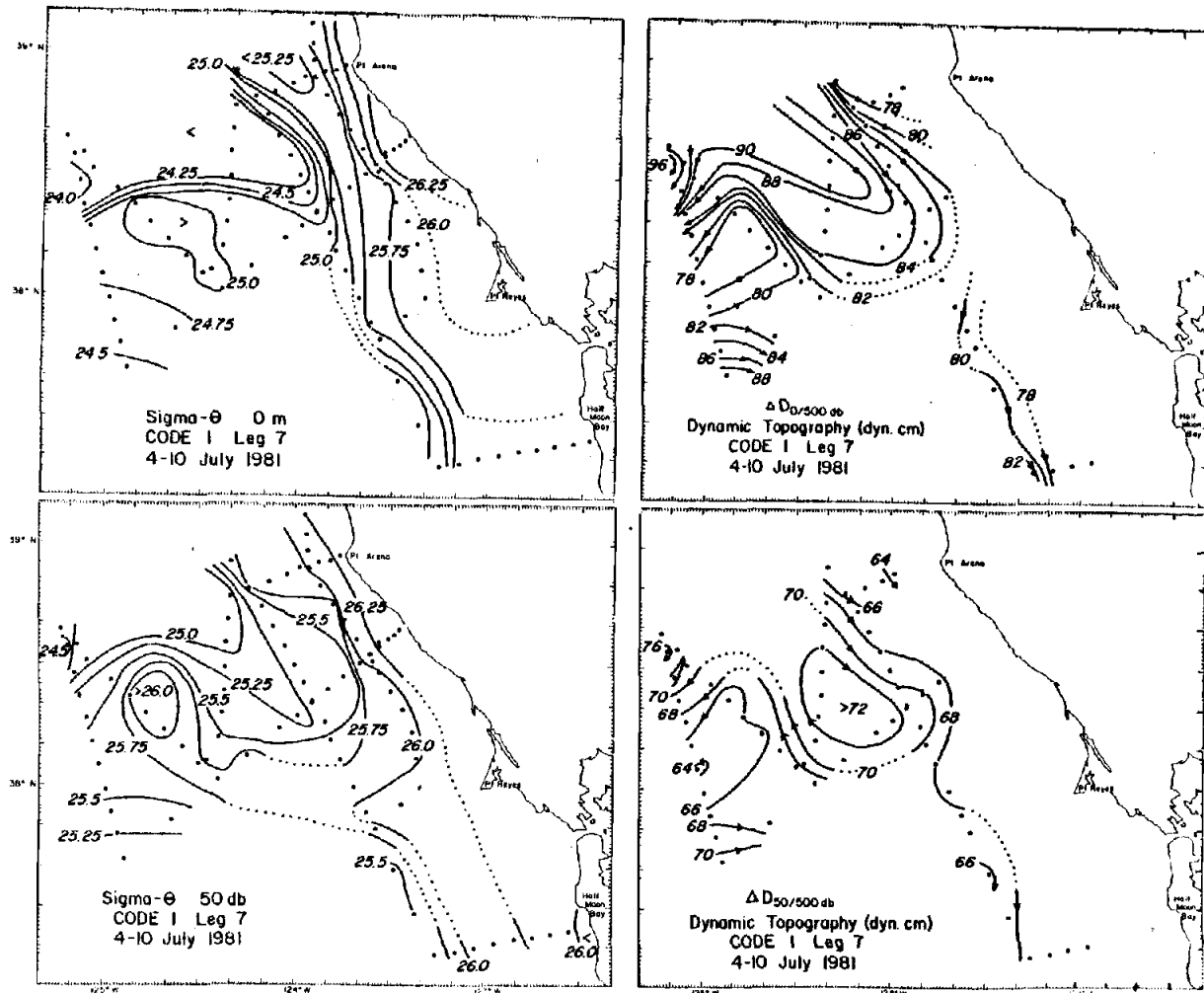


Figure 8

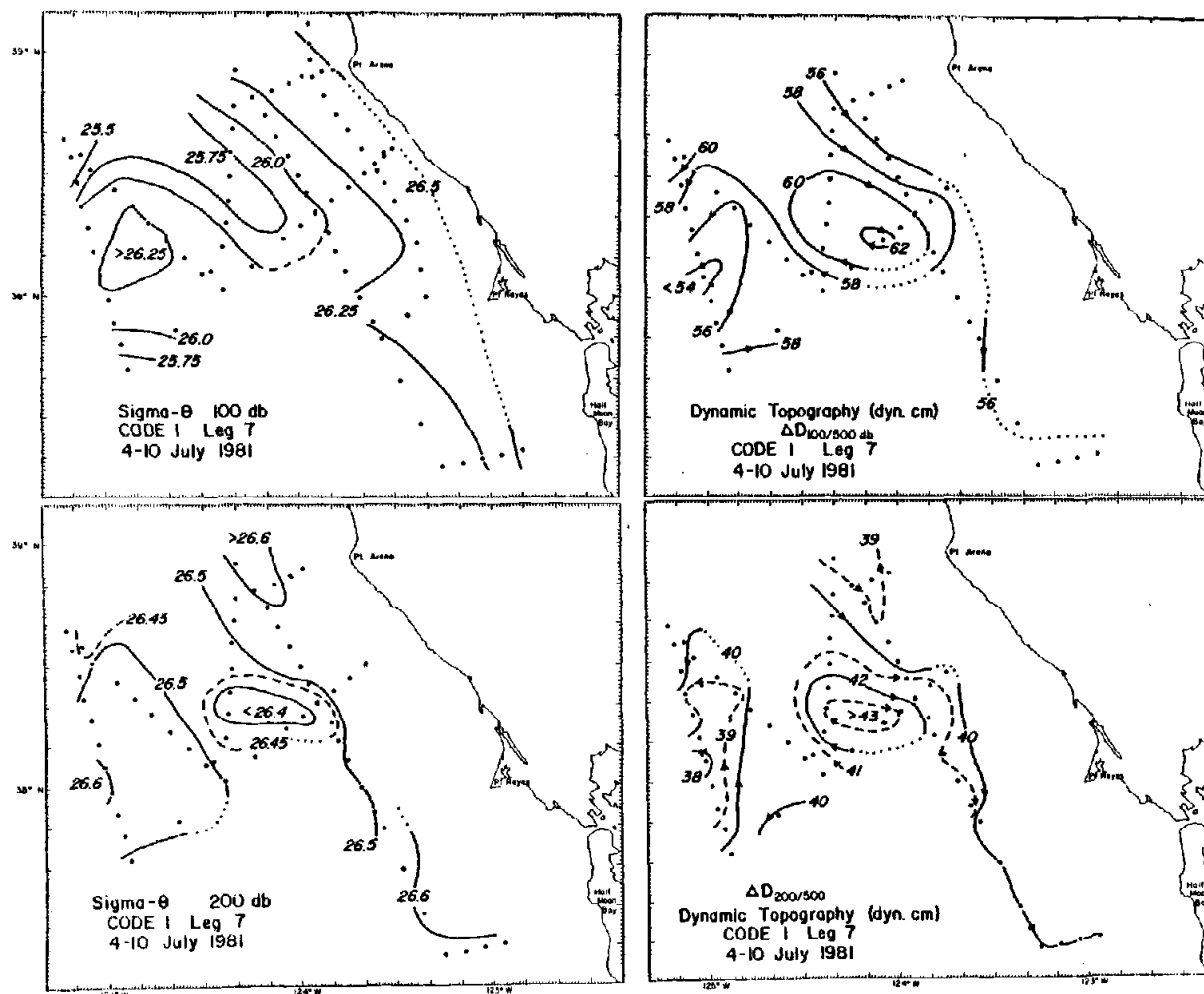


Figure 8 (cont.)

temperature, salinity and density distributions resemble those at 50 db. The tongue of relatively low salinity at 100 db lies directly under those at 50 db and the surface; the relatively high temperature and low density tongues extend somewhat farther south than at the shallower depths. Very dense ($\sigma_\theta > 26.5$) water with temperatures below 8.5°C and salinities about 34.0‰ are observed along the coast. At 200 db, the low salinity water still lies directly under the low-salinity tongues observed at shallower depths, but there is no corresponding tongue of high temperatures; instead, there is a local temperature maximum at about $38^\circ 10'\text{N}$, $124^\circ 10'\text{W}$, which lies under the southeast end of the warm tongue at 100 db. The density minimum ($\sigma_\theta < 26.4$) is at the same location as the temperature maximum.

The maps of temperature and salinity show that whereas the location of the area of the maximum temperature seems to change with depth, the area of the salinity minimum seems to stay at roughly the same location at all depths, at least in the upper 200 db. This implies that the T-S relationship changes with depth, and this is actually observed (Figure 6). At the sea surface there is a good linear relationship between temperature and salinity, if the Half Moon Bay stations are excluded. At 50 db, there is still a linear relationship between temperature and salinity, the Half Moon Bay stations are not distinct from the others at this depth. At 100 db the relationship is still linear but the salinity range is considerably reduced, and at 200 db the water is comparatively uniform.

Distributions of specific volume anomaly (δ) would show identical patterns to those seen in the distributions of the density anomaly (σ_θ) in Figure 8 since they are alternative representations of the density field. Since these distributions change significantly with depth, we would also expect the distribution of dynamic height (ΔD) to vary with depth, as ΔD is just the integral of the specific volume anomaly between two pressure surfaces p_1 and p_2 , i.e.,

$$\Delta D_{p_1/p_2} = \int_{p_1}^{p_2} \delta \, dp$$

The distribution of dynamic height relative to 500 db for the 63 stations having sufficient depth are shown in Figure 8; these do show significant variation with depth. The relative maximum at the sea surface occurs at about 38°38'N, 124°20'W, approximately 70 km southwest of Pt. Arena; at 200 db it occurs at about 38°17'N 124°12'W, i.e., about 40 km farther south. At each depth, the location of the density minimum almost coincides with the maximum in dynamic height (Figure 8); this coincidence occurs also at 150 and 300 db (Olivera et al., 1982, p. 69, 73). At the sea surface ΔD correlates very well with both temperature and salinity (the correlation coefficient, r , is 0.74 in both cases); at 200 db it correlates well with temperature ($r = 0.80$) but not at all with salinity ($r = 0.0$). This suggests that the effects of salinity are important only in the upper layers, where large gradients occur.

Lines of constant height can be interpreted as dynamic streamlines if the velocity field is assumed to be geostrophic, and if there are zero or very low velocities at the reference level. The streamlines in Figure 8 indicate strong southeastward flow off Pt. Arena; it is strongest at the surface and decreases rapidly with depth. This flow makes a sharp turn seaward somewhat south of the CODE Central Line (at about $38^{\circ}15'N$, $124^{\circ}W$) to become northwestward and then seaward. Farther south, at about $37^{\circ}50'N$, $125^{\circ}W$, flow toward the coast can be observed. Thus, two turns or gyres are detected, one is anticyclonic, around the relative maximum in dynamic height at $38^{\circ}40'N$, $124^{\circ}20'W$; the other is cyclonic, around a minimum in dynamic height at $38^{\circ}10'N$, $125^{\circ}W$, due southwest of the maximum. The surface flow off San Francisco Bay seems to be southeastward, although there is not sufficient data to be conclusive.

The large horizontal gradients in dynamic height, and therefore the stronger geostrophic currents, correspond to large horizontal gradients of temperature, salinity, and density at the sea surface. At deeper levels, the flow pattern remains almost the same, with smaller gradients, i.e. lower velocities. Even at 200 db it is still possible to identify the two gyres, the northwestward flow separating them, and the equatorward flow near the coast.

IV. Discussion

A. The Water Masses:

The temperature-salinity (T-S) characteristics of the California Current lie between two extreme water masses, the Subarctic Pacific and the Eastern Equatorial Pacific, with a transition zone off California (Tibby, 1941; Sverdrup et al., 1942). Within this range, changes in the surface properties usually occur due to the influence of atmospheric factors and continental run-off. The distribution of temperature and salinity in July 1981 show that two main surface water masses are present off Pt. Arena; one relatively warm and fresh and another cooler and more saline, both separated by a strong density front (Figure 5).

The T-S diagram constructed with surface values of the CTD stations shows a high correlation between these two properties (Figure 6a). Stations with surface values above 13°C and below 32.80‰ were made northwest of the density front, whereas those with greater salinity values were made southeast of it, near the coast. A group of ten stations with relatively high temperature and salinity (above 11.5°C and 33.80‰) were occupied near the coast. They are Stations 9-11 of the first Central Line and 104-111 occupied off Half Moon Bay. They indicate the presence of a third water mass whose high salinity is characteristic of the coastal waters and whose high surface temperature may be due to local heating. It is interesting to point out that when these stations were

made, the wind was not strong near the coast (Figure 4). At 100 db, there is still a linear tendency in the T-S distribution (Figure 6c). At this depth, the T-S points are clustered between 8°C - 10°C and 33.50‰ - 34.00‰ ; however, stations north of the frontal area still have low salinity, in particular Station 33 (11°C - 32.90‰). There is no linear tendency at 200 db (Figure 6d) which suggests that the lighter water mass is constrained to the upper layers.

The T-S diagrams of stations within the warm-fresh water area are very similar to those of stations occupied farther north along $41^{\circ}43'\text{N}$ off Crescent City in July 1967 (Barstow et al., 1969) (Figure 9). These stations are clearly influenced by the Columbia River plume, as indicated by low salinity values in the upper layers (Cissel, 1969). The discharge of this river is characterized by a major sustained peak at this time of the year from interior snow-melt (Barnes et al., 1972). The similarity of the T-S diagrams is particularly evident in the upper 50 db where relatively warm (above 13°C) and fresh (salinity below 32.80‰) water is observed. The subsurface temperature distribution indicates the warm water mass has almost disappeared at 50 db and there is no trace of it at 100 db (Figure 7). Its low salinity content, its shallowness and high correlation with data from the Oregon-California border, lead to conclude it is a dilute remnant of the Columbia River plume, advected southward by the California Current. This is consistent with observations by Barnes et al. (1972) who established a quasi-steady-state region of dilution of the Columbia River waters during summer, in which the isohaline of 32.50‰ reaches $40^{\circ}30'\text{N}$.

Figure 9

T-S diagrams of stations KP58, KP59 and KP60 made in July 1967 (bigger dots in the inset); and those of stations 34 and 49 made in July 1981. The inset shows the sea surface salinity off Oregon in July 1967 (after Cissell, 1969).

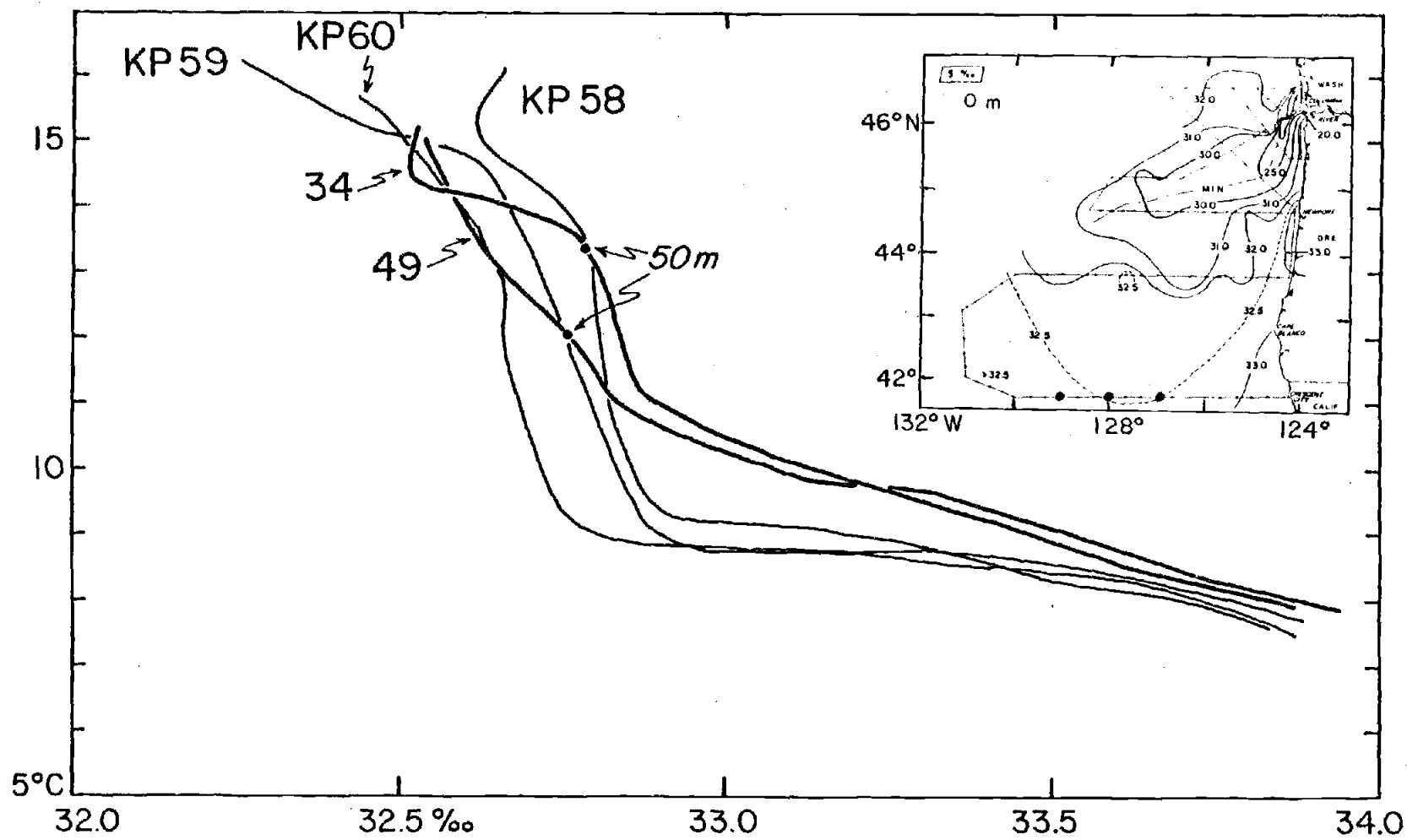


Figure 9.

The T-S characteristics of the nearshore waters seem to be related to the general circulation in this particular area at this time of the year. This circulation includes upwelling of subsurface colder and saltier water along the coast when the wind stress causes offshore transport in the surface layer (Smith, 1968). The time series of wind speed and direction measured during the CTD stations (Figure 4), show winds were upwelling favorable throughout the cruise. Winds were weaker at the beginning, during the first Central Line, than during the remainder of the cruise. The vertical sections of temperature indicate that nearshore water above 100 m became colder within the four days between 4-5 July and 8 July (Figure 10); winds averaged about 25 kts on 7 July (Figure 4). Moreover, as a result of ascending water from subsurface levels, the thermocline and the halocline both slope upward toward the coast, and there is a decrease of vertical temperature and salinity gradients inshore (Figure 10). The T-S diagram constructed with surface values of Stations 71 through 80 is very similar to the T-S curve of Station 22 (Figure 11). There is a definite similarity between the T-S properties at the surface at Stations 71-76 and those in the water column between 80 and 160 db at Station 22; although the surface values have temperatures about 0.5°C warmer, probably due to local heating, this similarity suggests that the surface water near the coast has upwelled from depths between 80 and 160 m.

In summary, three surface water masses are identified, a warm and fresh, with influence of the Columbia River plume; a

second cooler and more saline originated at the coast by upwelling and extending seaward; and a third near the coast too, but warmer and with high salinity, probably a consequence of local heating of the upwelled water (Figure 12).

Figure 10

Vertical sections of temperature and salinity along the
CODE Central Line for 4-5 July and for 8 July 1981.

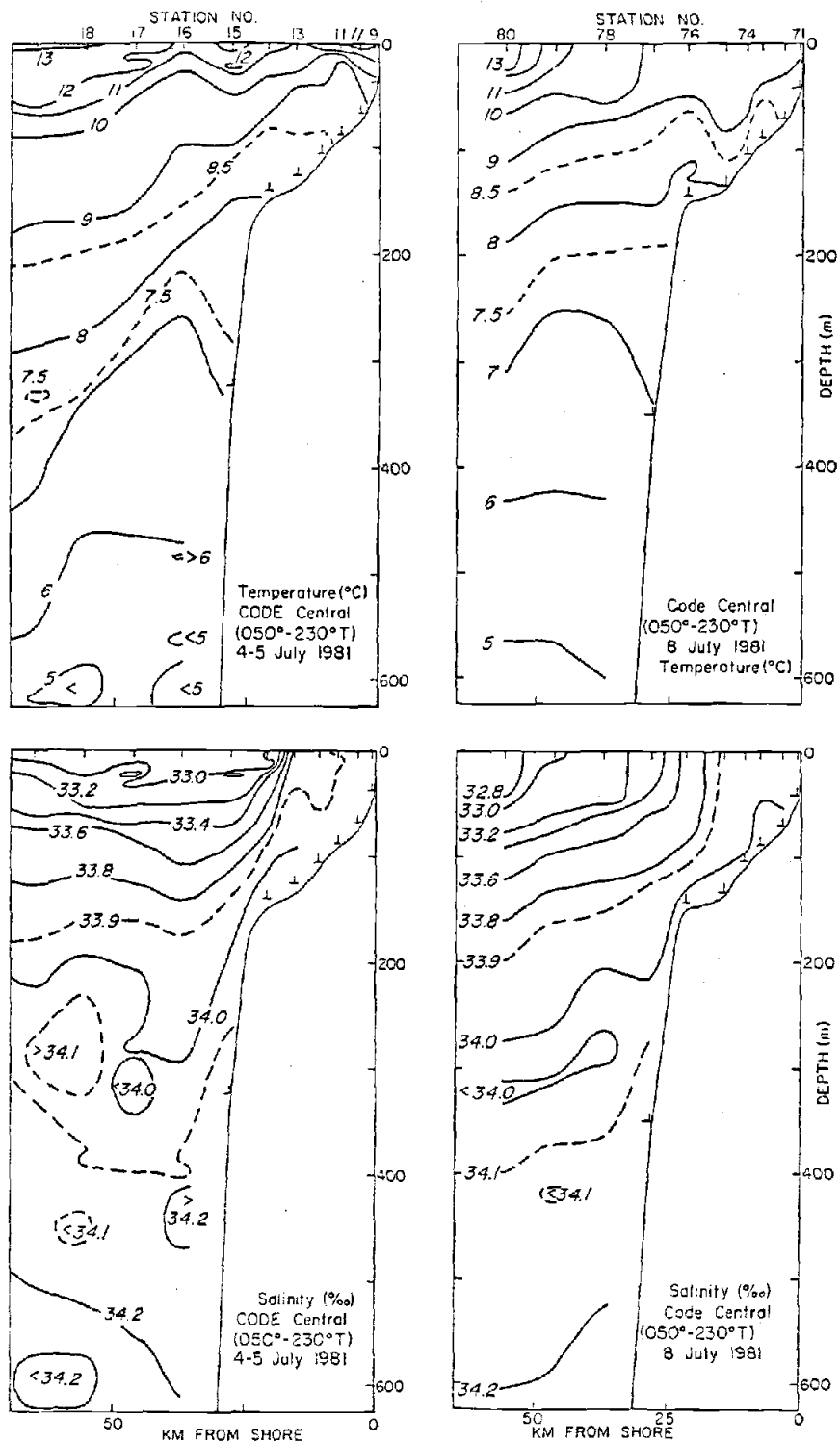


Figure 10.

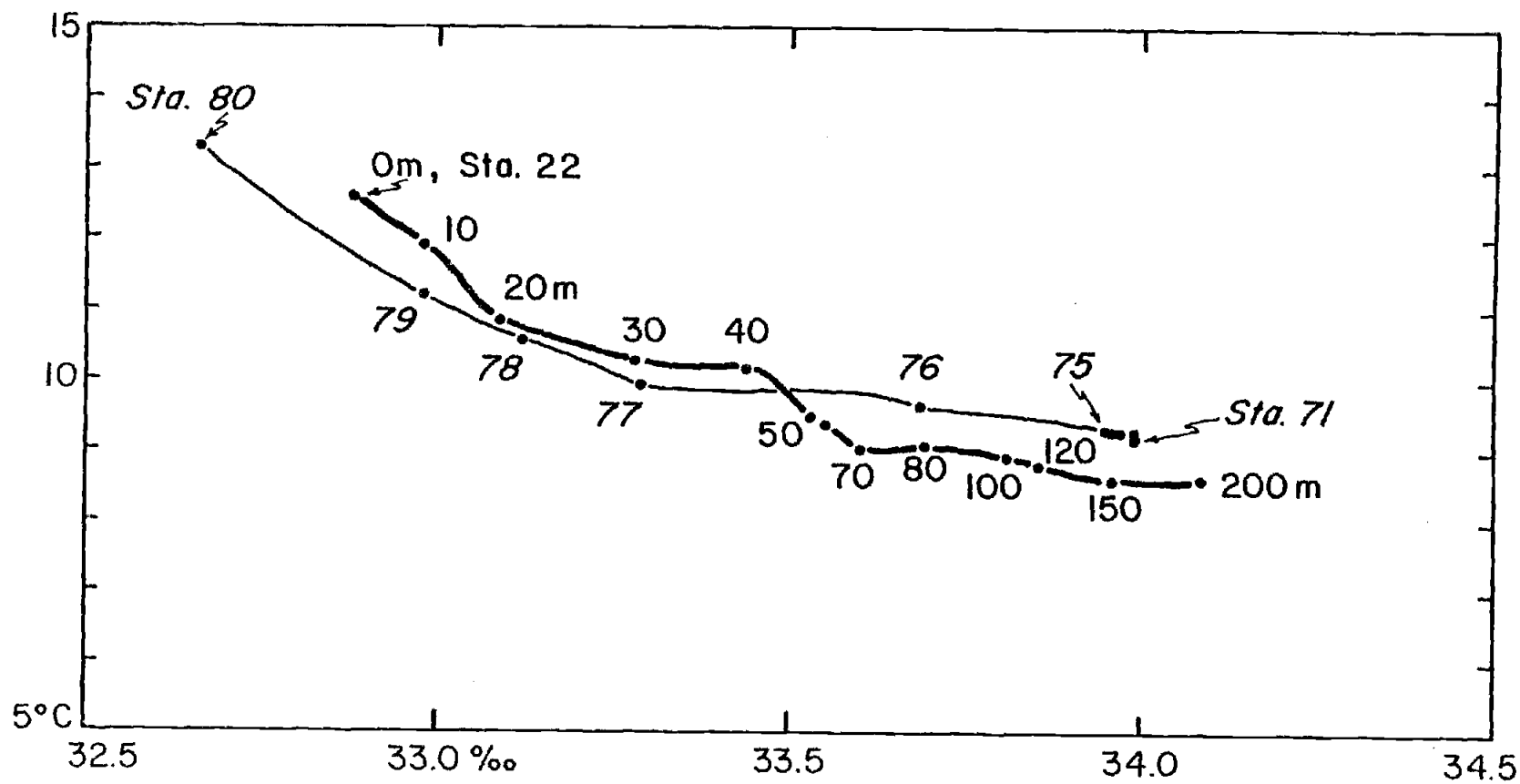


Figure 11. T-S diagram of station 22 up to 200 m and that constructed with surface values of stations 71 through 80.

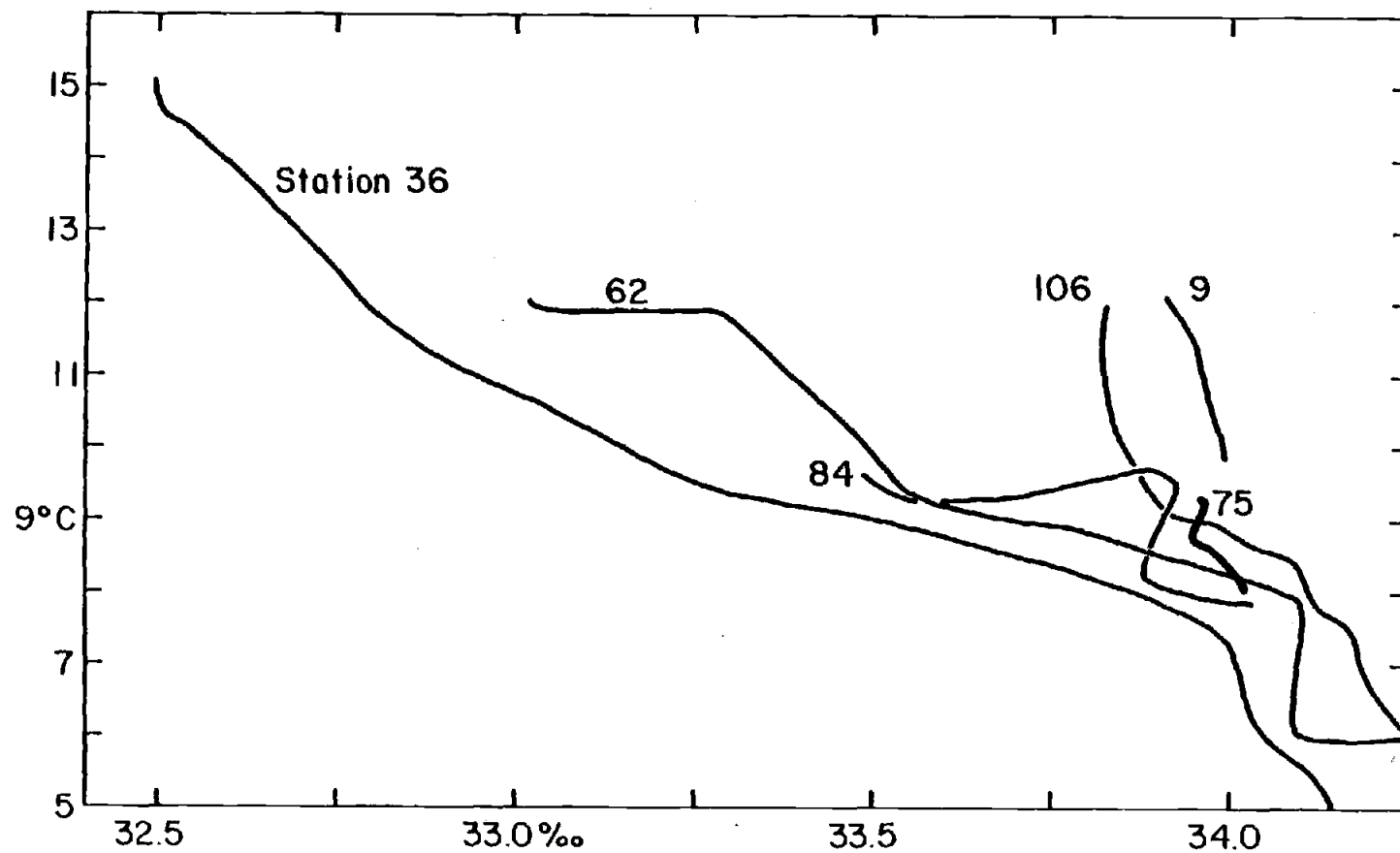


Figure 12. T-S diagrams of stations occupied within the warm and fresh water (station 36), within the cool and saline water (station 75), and within the warm and saline water (stations 9 and 106). Additional diagrams for stations 62 and 84 lie within a transition area.

B. The Distribution of Water Masses and the Related Circulation:

T-S sections, in which isohalines map the distribution of salinity as a function of temperature and horizontal distance, show the changes in the thermohaline characteristics along a hydrographic section (Bruce, 1981) (Figure 13). The isohalines will have zero slope where no change of T-S characteristics occur, i.e. within a particular water mass. Isohalines will slope either up or down wherever there is a change in T-S characteristics, i.e. at a boundary between different water masses; the steeper the slopes, the sharper the water mass boundary. Likewise, T- V_g sections (isotachs plotted as a function of temperature and horizontal distance) show the changes in the geostrophic velocity field with respect to temperature along a hydrographic section (Figure 13). By studying T-S and T- V_g sections together, it is possible to determine whether there is a relationship between the water mass structure and the velocity field.

The T-S section for Stations 24-34 (Figure 13a) shows two major changes in the alongshore distribution of temperature and salinity. The first takes place between Stations 32 and 30: it is indicated by a sharp surface temperature gradient (from 15.4°C to 13.2°C within 20 km); at the same location, the isohalines bend sharply upwards. Both gradients indicate the boundary between two water masses. The T- V_g section corresponding to these stations shows that at this boundary, strong geostrophic flow directed seaward is found. The second change is observed between Stations 25-27:

although the temperature gradient is smaller, the slope of the isohalines is still sharp. Relatively strong geostrophic flow directed toward the coast is found here.

A clear example of the correspondence between the T-S and T- V_g sections can be seen in the sections for Stations 34-43 (Figure 13b). The strong surface temperature gradient between Stations 38-39 together with the sharp slope of the isohalines marks the boundary between the warm-fresh and the cool-saline water masses. They are associated with a strong seaward geostrophic flow of 88 cm sec^{-1} . South of the frontal region, the surface temperature and the isohalines do not show abrupt variations, which is consistent with the weak flow at the same location.

The frontal region separating the two water masses described in the previous discussion is also depicted by the surface temperature gradient and sharp sloping of isohalines in the sections for Stations 52-43 and 52-64, (Figure 13c,d) closer to the coast. These two sections present similar characteristics: a positive surface temperature gradient in the northern part which is associated with strong geostrophic flow toward the coast and a negative one farther south which is associated with a weaker flow directed offshore. In both cases, there is a clear indication that the stronger geostrophic velocities correspond to major changes in both temperature and salinity, i.e., with a boundary between water masses.

The same characteristics, although with considerably smaller T-S variations, are observed along the Central Line (Stations 9-24,

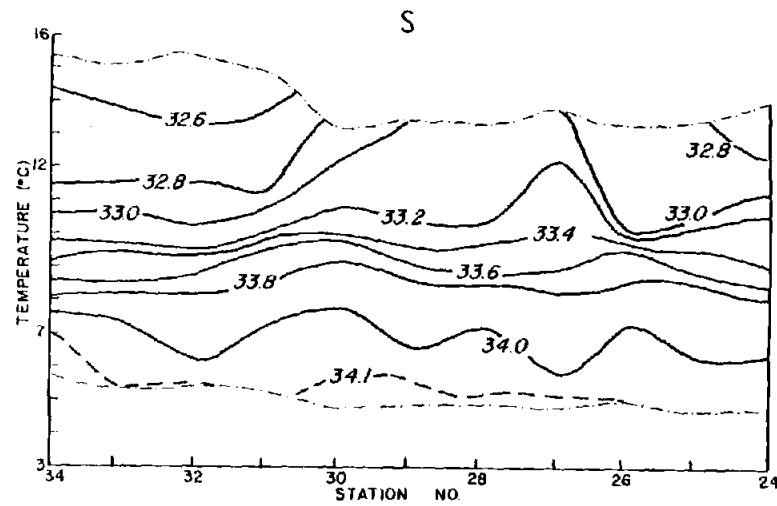
Figure 13e), where the direction of the flow is again consistent with the sign of the surface temperature gradient and the slope of the isohalines.

It is interesting to note that the opposite slope of the line indicating surface temperature and the isohalines at the frontal areas, result in strong density gradients between stations bounding the distinct water masses (Figure 7 and 8). One should expect smaller density gradients, i.e., lower geostrophic velocities where temperature and salinity compensate one another in determining the density field (see section 52-64, between Stations 58-60).

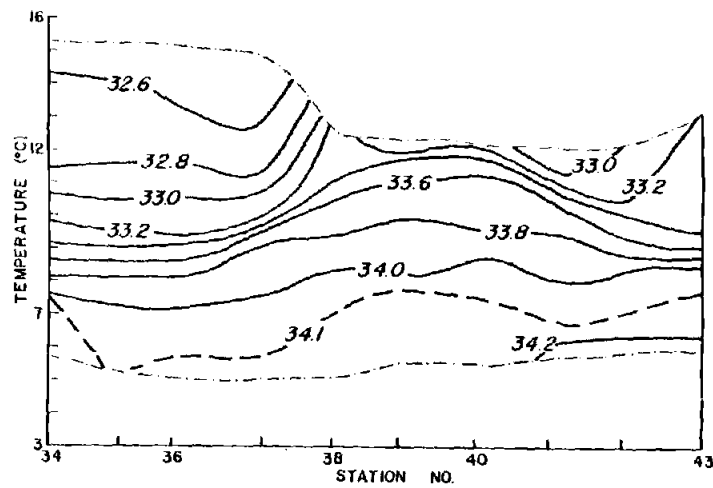
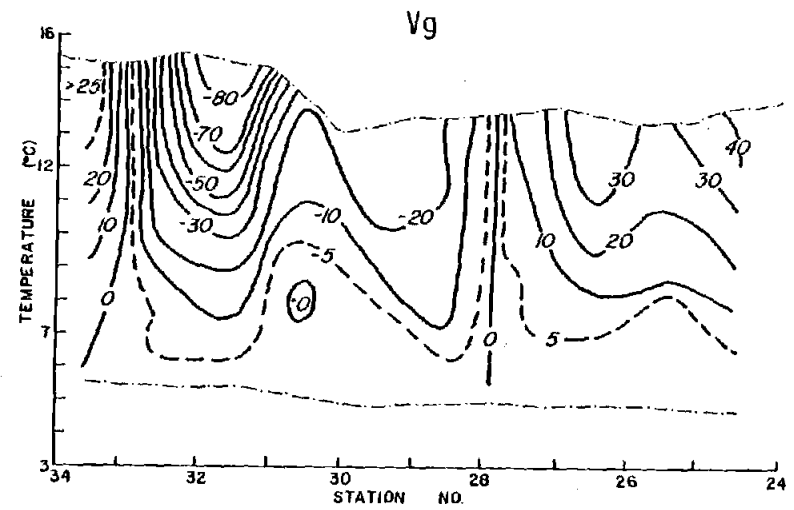
Summarizing, the T-S and T- V_g sections in this area identify the frontal area separating two distinct water masses. Further, they show that the strong geostrophic flow is associated with this region, i.e., the circulation is primarily along the water masses boundaries. The near symmetry of the T-S structure along sections 24-34 and 34-43 (about Stations 28 and 40, respectively) is consistent with a cyclonic flow around the westernmost part of the cool-saline water mass. Likewise, the symmetric features along sections 43-52 and 52-64 (about Stations 50 and 56, respectively) confirm the existence of the anticyclonic gyre closer to the coast, i.e., alternating zones of southeastward-northwestward flow.

Figure 13

Temperature-Salinity (T-S) and Temperature-Geostrophic Velocity (T-Vg) sections for: (a) stations 34-24; (b) stations 34-43; (c) stations 43-52; (d) stations 52-64; and (e) stations 9-24. The geostrophic velocity is with respect to 500 db (in cm/sec). Dashed lines represent temperature at the sea surface and at 500 db.



(a)



(b)

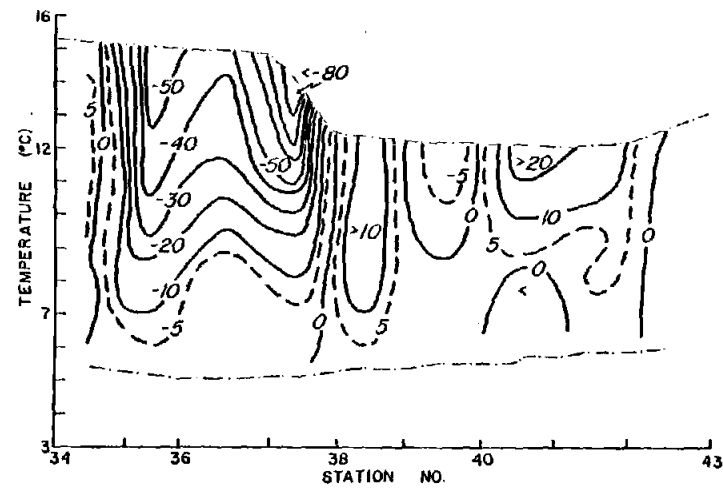
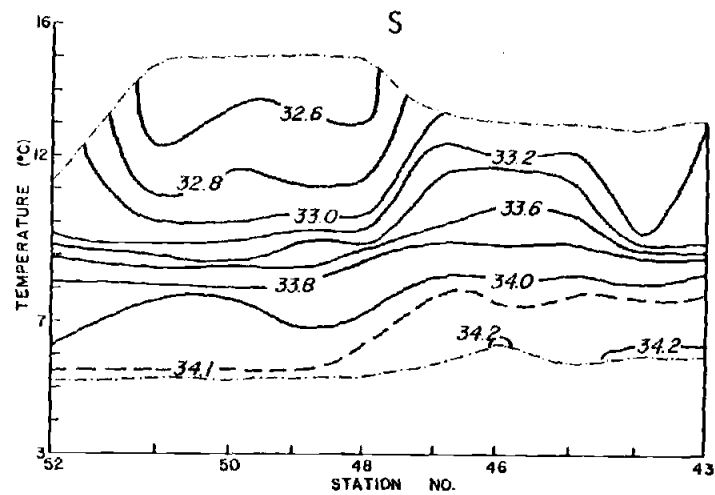
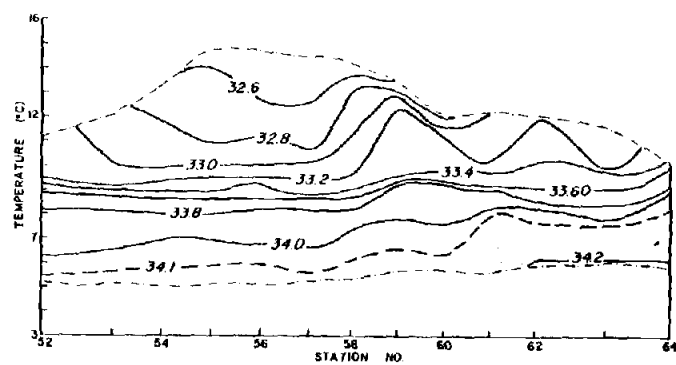
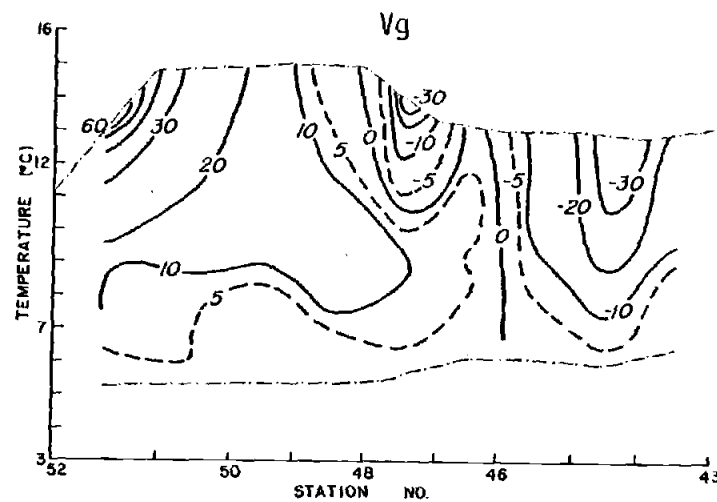


Figure 13



(c)



(d)

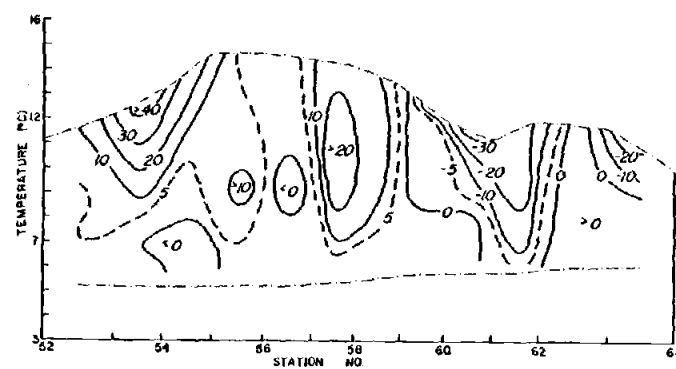
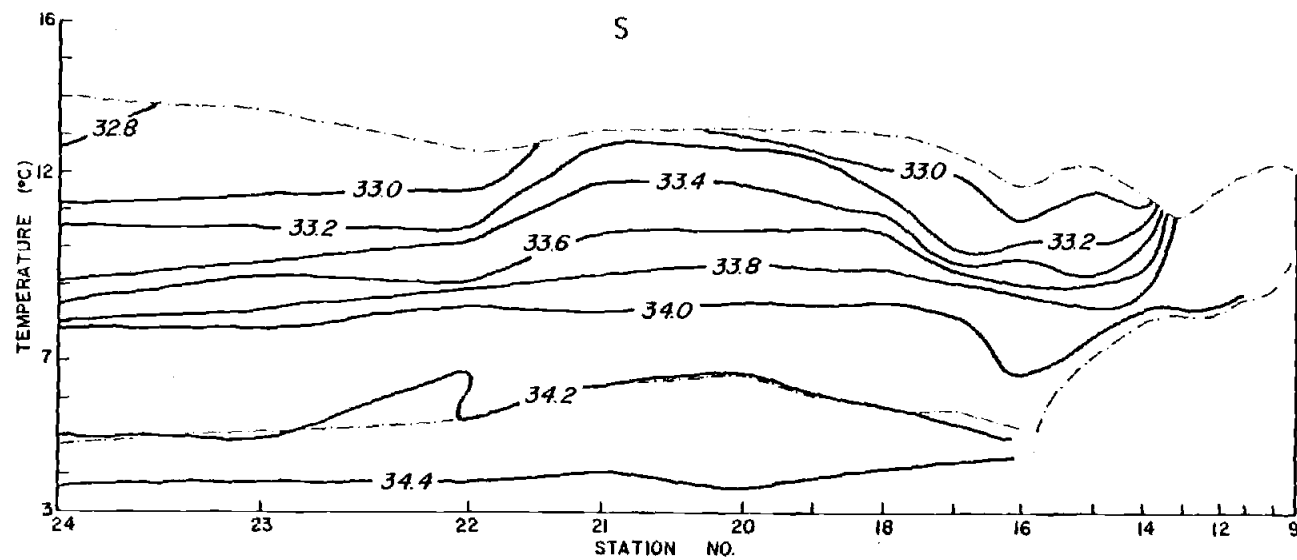


Figure 13 (cont.)



(e)

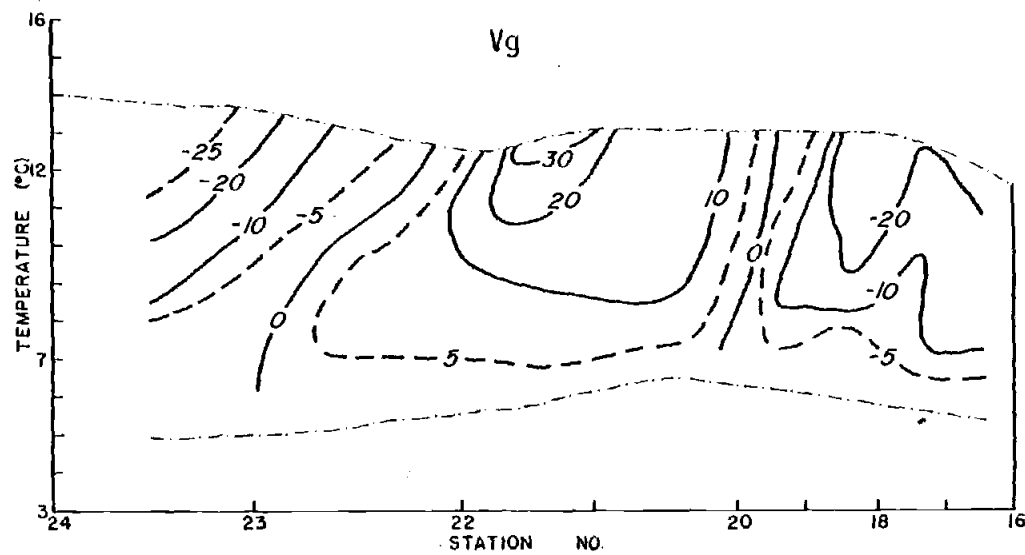


Figure 13 (cont.)

C. Large Scale Circulation:

The California Current and the California Undercurrent are comprised in the California Current System. While California Current refers to the equatorward flow, California Undercurrent refers to the subsurface poleward flow over the slope (Hickey, 1979). Reid et al. (1958) apply the term California Current to all southward flow in the North Pacific gyre. Hickey (1979) concluded that the California Current has both an offshore and a nearshore maximum and that the seasonal variation of the nearshore flow appears to be related to the seasonal variation of the alongshore component of the wind stress at the coast. In her work, she also concluded that: "large-scale flow separation in the vicinity of headlands may account for the occurrence of late summer and fall undercurrents that appear as large anomalies from the wind-driven coastal flow south of 40°N". Other studies agree on the seasonal variation of the currents (Jones, 1918; Collins and Pattullo, 1970; Wyatt et al., 1972; Huyer et al., 1975). They found that during summer, when northerly wind prevails, the direction of the current tends to be southward, whereas during winter, the current flows northward, consistent with prevailing southerly wind.

The observations in the CODE area, off Northern California, confirm what is concluded by Hickey. The flow south of Pt. Arena is primarily southward with a strong geostrophic jet parallel to the coast (Figure 8), which is consistent with the southeastward winds. Furthermore, a surface counterflow is detected farther

offshore; this counterflow is also present at 100 and 200 db (Figure 8). It seems not to be related with the California Undercurrent but it appears to be a subsurface expression of the anomalous countercurrents pointed out by Hickey. The low dynamic heights found near the coast, associated with cool-saline water, increasing seaward, are consistent with those computed by Hickey (1979) from data given by Wyllie (1966) (compare Figures 8 and 14), although we found higher values at locations much closer to the coast.

Indications of poleward flow were found over the continental slope (Figure 15). Off Half Moon Bay ($37^{\circ}20'N$) a northward undercurrent flows between 100 db - 300 db with maximum velocity of 4 cm sec^{-1} at 150 db. Farther north, off Pt. Arena ($39^{\circ}N$), the poleward flow is detected deeper, between 225 db - 500 db, with a maximum velocity at 350 db of 6 cm sec^{-1} . However, no such flow was found in between those locations at $38^{\circ}30'N$ (along the Central Line).

Estimating the mean alongshore currents from stations with the greatest possible separations yields surface current estimates of $\sim 10 \text{ cm/sec}$ (Figure 16). These station separations are about twice as great as those used by Hickey to obtain estimates of the mean currents of about 5 cm/sec i.e., the larger alongshore flow in July 1981 was stronger than Hickey's estimates of the mean flow off Pt. Arena.

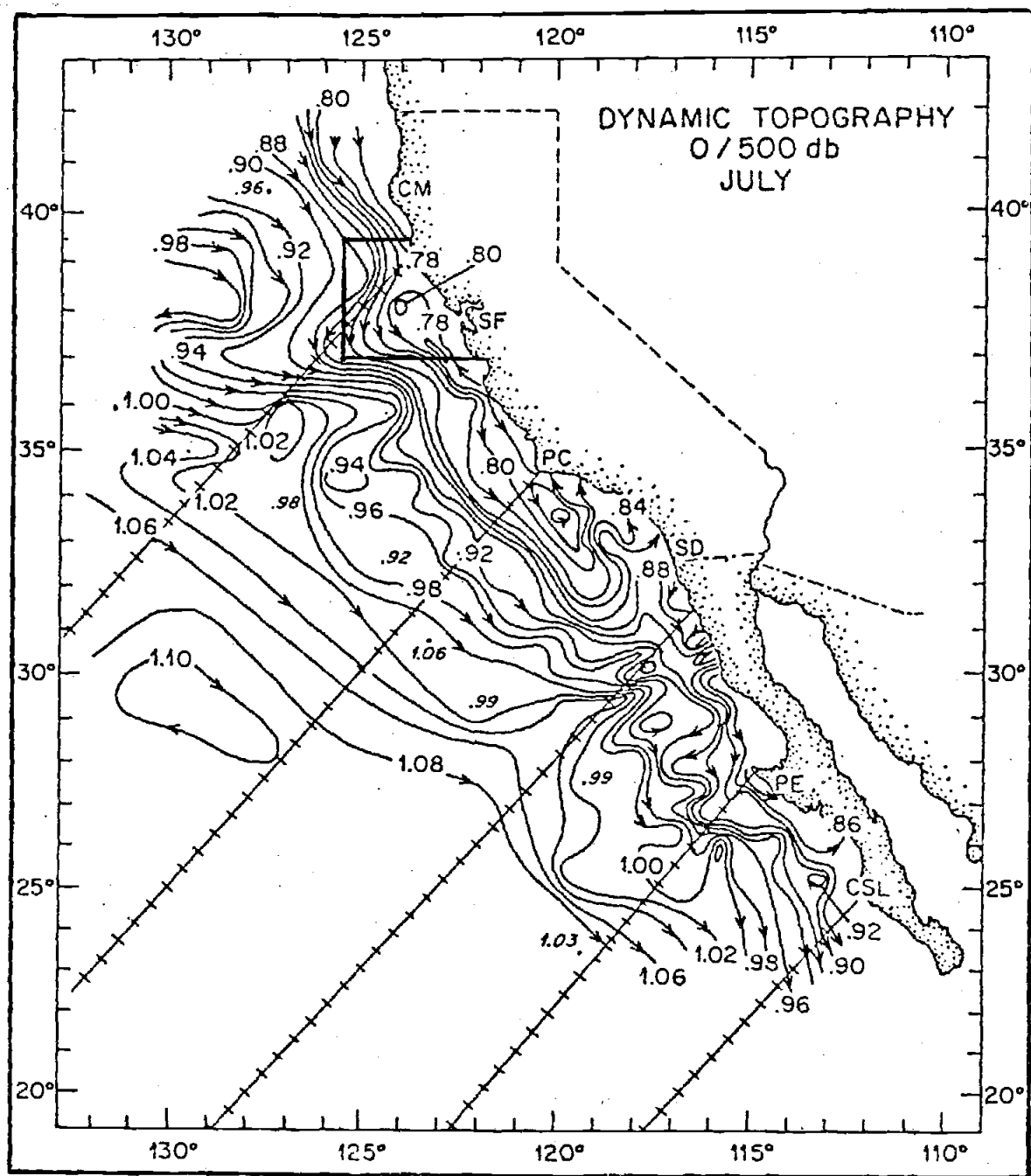


Figure 14. Mean dynamic topography of the sea surface off California relative to 500 db during July. Contour intervals are 0.02 dynamic meters (after Hickey, 1979). The squared region represent the CODE 1- Leg 7 survey area.

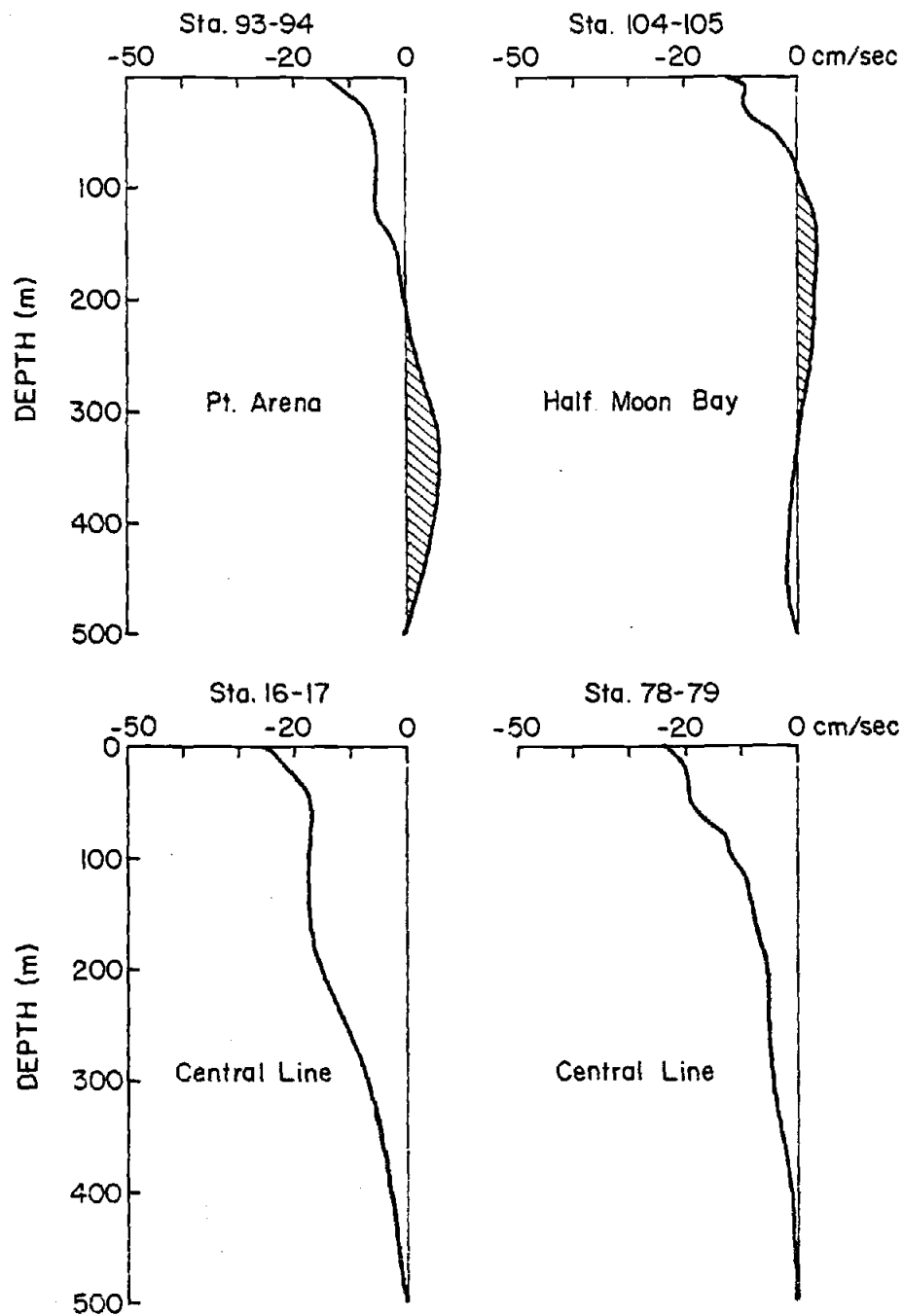


Figure 15. Geostrophic velocity profiles relative to 500 db for pairs of stations near the continental slope. Shaded areas and negative values represent poleward and equatorward flow respectively.

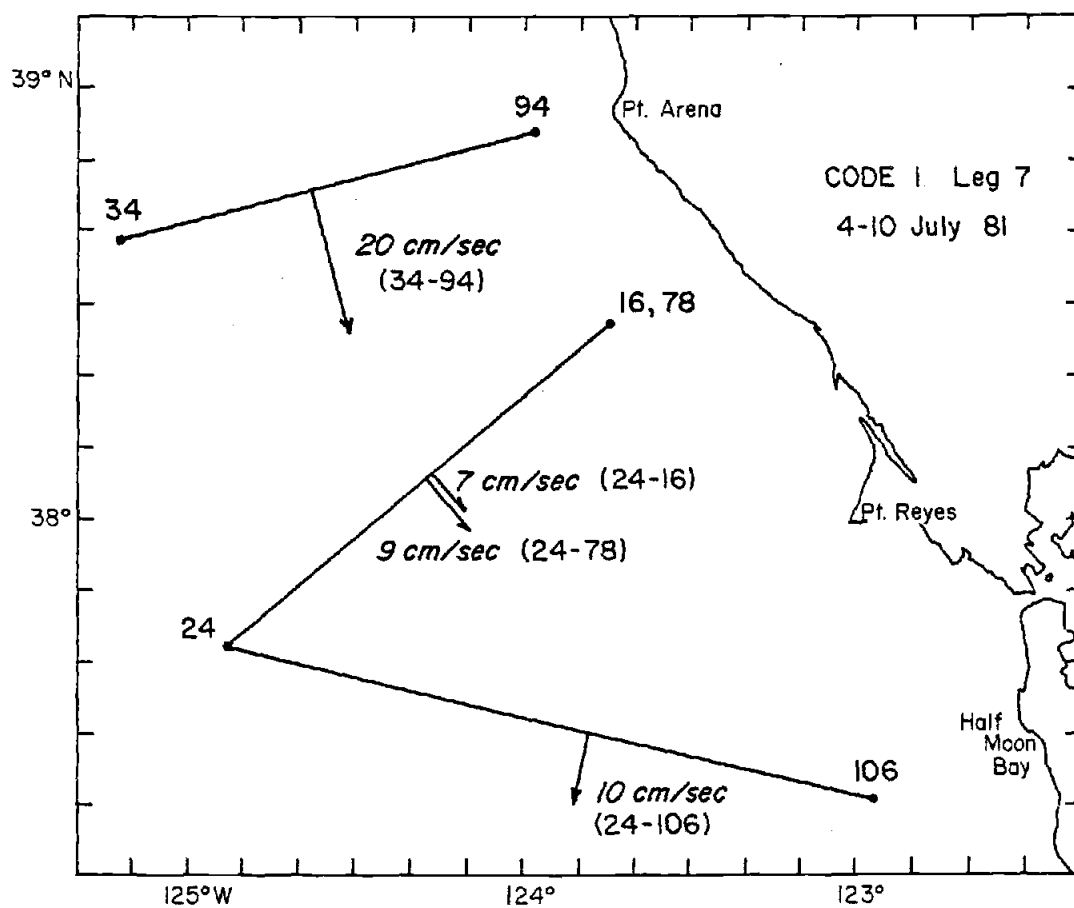


Figure 16. Geostrophic velocity at the sea surface relative to 500 db between distant stations.

D. Comparison of Geostrophic and Observed Currents

During the cruise, personnel from Scripps Institution of Oceanography operated a Doppler Acoustic Log which measured the velocity of water beneath the ship's hull relative to the ship. By recording the ship's position, absolute velocities can be computed for the water at a depth of about 30 m. Figure 17 shows a map of these measured vectors (courtesy of Michael Kosro, SIO), and the dynamic topography at 30 db. In general, the vectors lie very nearly parallel to the geostrophic streamlines, and vector magnitudes are greatest where the streamlines lie closest together. A quantitative comparison for a few selected locations indicates that the geostrophic currents have the same order of magnitude as the measured currents.

The highest velocities at the sea surface, as determined from the gradient of dynamic heights, are also found in regions where the vectors (at 30 m) are largest, i.e. at the frontal areas (Figure 8). The strongest flow was detected at the sea surface off Pt. Arena, running southward at approximately 52 km from the coast in a band about 11 km wide, with a velocity of 96 cm/sec. Strong westward flow of 88 cm/sec was found farther offshore, also associated with the front. Indications of surface northwestward flow of about 45 cm/sec were observed offshore (Figure 8), decreasing with depth. Off Half Moon Bay, off the continental shelf, the surface geostrophic velocity was 65 cm/sec, equatorward. The qualitative comparison of the results of both methods shows that the geostrophic approximation describes fairly well the circulation pattern.

Figure 17

Maps of currents velocity: (top) as measured by a Doppler Acoustic Log (courtesy of Michael Kosro, Scripps Institution of Oceanography); (bottom) as observed in the dynamic height of 30/500 db (contour intervals are 2 dyn cm).

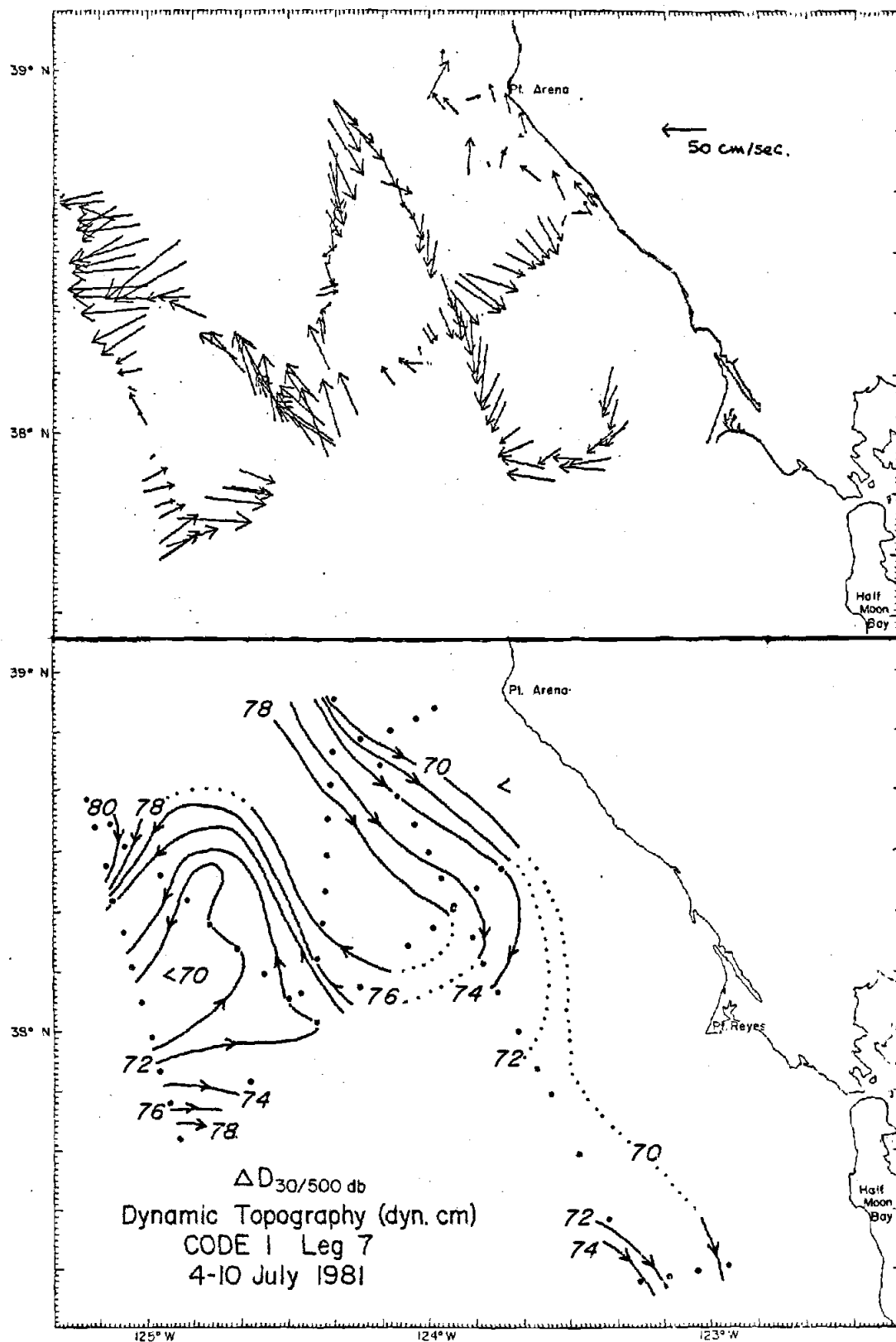


Figure 17

V. Summary and Conclusions

Two water masses were identified, separated by a strong density front, off Northern California. Their T-S properties show a rather complex distribution, characterized by surface and subsurface meandering of isotherms, isohalines and isopycnals. The satellite imagery and the Sea Surface Thermal Analysis charts show a cold water body extending from the coast offshore, intruded in its northwestern edge by a warmer water mass. The hydrographic observations were very consistent with the satellite data and provided evidence for the existence of both water masses. The position of the resulting density front bounding them was determined by five ship crossings through areas with large surface horizontal density gradients. The position so determined agrees remarkably well with the position observed in the pictures taken by the satellite while the cruise was in progress. The front separates a high in dynamic sea surface topography, centered near $38^{\circ}31'N - 124^{\circ}19'W$, from a low located farther southwest, centered near $38^{\circ}13'N - 124^{\circ}50'W$; both associated with the warm and the cold waters respectively. The distribution of temperature and salinity shown through the T-S sections and the T-S diagrams, indicates the cool water has relatively high salinity, which explains its very high density. This water is of subsurface origin. The warm water, on the other hand, has low salinity. The T-S diagrams and the thermohaline vertical distribution led to conclude this warm-fresh water is a dilute remnant of the Columbia River plume, which due to its very low density,

is constrained to the upper 50 and 70 db. A third water mass, relatively warm and saline, was detected near the coast. The T-S distribution seems to indicate that this was upwelled water locally heated.

The water circulation in the upper 500 db is characterized by a very complex pattern, which is similar to those in the distributions of temperature and salinity. The geostrophic velocity sections and dynamic topography maps display alternating zones of southeastward and northwestward flow as well as westward and eastward flow. The strongest flow was found at the sea surface along the boundary between the warm-fresh and the cool saline water masses. Evidence was found of a subsurface counterflow of about 5 cm/sec, near the continental slope, off Pt. Arena and off Half Moon Bay. At the same locations but at the sea surface, the flow was clearly southward. However, no evidence of such counterflow was found near the slope along the Central Line. This seems to indicate that the subsurface northward flow was not continuous.

VI. Bibliography

- Allen, J.S., Upwelling and coastal jets in a stratified ocean,
J. Phys. Oceanogr., 3, 245-257, 1973.
- Barnes, C.A., A.C. Duxbury, and B.A. Morse, Circulation and
selected properties of the Columbia River effluent at sea,
In: The Columbia River Estuary and Adjacent Ocean Waters-
Bioenvironmental Studies, University of Washington Press,
Seattle.
- Barstow, D.W., W. Gilbert, and B. Wyatt, Hydrographic Data from
Oregon Waters 1967, Ref. 69-3, Oreg. State Univ., Sch. of
Oceanogr., Corvallis, 1969.
- Bruce, J.G., A note on some uses of θ -S sections, J. Geophys. Res.,
86, 6649-6652, 1981.
- Burt, W., and B. Wyatt, Drift bottle observations of the Davison
Current off Oregon, Studies in Oceanogr., 156-165, 1964.
- Cissel, M.C., Chemical features of the Columbia River plume off
Oregon, M.S. thesis, Oreg. State Univ., Corvallis, 1969.
- Collins, C.A., and J. Pattullo, Ocean currents above the continental
shelf off Oregon as measured with a single array of current
meters, J. Mar. Res., 28, 51-68, 1970.
- Hickey, B.M., The California Current System - hypotheses and facts,
Progress in Oceanogr., 8, 4, 191-279, 1979.
- Huyer, A., and R.L. Smith, A subsurface ribbon of cool water over
the continental shelf off Oregon, J. Phys. Oceanogr., 4, 381-391,
1974.

- Jones E., The neglected waters of the Pacific coast, U.S. Coast and Geodetic Survey, Special Publication (48), 1918.
- Kelly, K.A., Infrared Satellite Data from the First Coastal Ocean Dynamics Experiment. March-July 1981, Ref. 82-15, Scripps Institution of Oceanography, La Jolla, 58 pp, 1981.
- Olivera, R.M., W. Gilbert, J. Fleischbein, A. Huyer, and R. Schramm, Hydrographic Data from the First Coastal Ocean Dynamics Experiment: R/V Wecoma, Leg 7, 1-14 July 1981, Ref. 82-8, Oreg. State Univ., Sch. of Oceanogr., 163 pp, 1982.
- Reid, J.L.Jr., G.I. Roden, and J.G. Wyllie, Studies of the California Current System, California Cooperative Oceanic Fisheries Investigations Progress Report, 7-1-56 to 1-1-58, Marine Resources Communications, California Department of Fish and Game, 27-56, 1958.
- Smith, Robert L., Upwelling, Oceanogr. Mar. Biol. Ann. Rev., 6, 11-46, 1968.
- Sverdrup, H.U., M.W. Johnson, and R.H. Fleming. The Oceans their Physics, Chemistry and General Biology, Prentice-Hall, New York, 1082 pp, 1942.
- Tibby, R.B., The water masses off the west coast of North America, J. of Mar. Res., 4, 112-121, 1941.
- Wyatt, B., W. Burt, and J. Pattullo, Surface currents off Oregon as determined from drift bottle returns, J. of Phys. Oceanogr., 2, 286-293, 1972.
- Wyllie, J., Geostrophic flow of the California Current at the surface and at 200 meters, California Cooperative Oceanic Fisheries Investigations Atlas #4, 288 pp, 1966.